

平成28年度 修士論文

Non-contact measurement of eyeblink by using Doppler
sensor

学籍番号 1532072

氏名 AMIR MALEKI

知能機械工学専攻 内田雅文研究室

指導教員 内田雅文 准教授

副指導教員 桐本 哲郎 教授

提出日 平成29年02月28日

**Non-contact measurement of eyeblink by using Doppler
sensor**

Amir Maleki

Graduate School of Informatics and Engineering

The University Of Electro-Communications

Master Thesis

March 2017

ドップラーセンサーを用いたアイブリンクの非接側定

論文要旨

自然界にはさまざまなゆらぎ現象が確認されるが、それらが統計的に完全に独立で不規則な過程を示すことは稀である。瞬目はヒトにとって極めて自然な運動の一つであり、認知科学、ヒューマンコンピュータインタフェース等に応用が期待されている。例えば認知科学の分野では、ヒトの数々の精神的かつ身体的な運動が $1/f$ ゆらぎの特性を示し得ることが確認され、多くの研究者がゆらぎ特性の意味することを見つけようと試みている。瞬目は車両および航空機運転者の眠気の探知に有効である為、瞬目の計測の重要性は高い。従来、瞬目の計測には EOG、赤外線センサ、カメラおよびドップラーセンサなどが用いられてきた。近年では、グーグルグラスのよう、赤外線センサなどの搭載されたセンサにより瞬目を計測可能な眼鏡型デバイスがいくつか提案されている。ドップラーセンサは、他の手法では問題となる長距離での検出などいくつかの長所がある。故に、本研究ではドップラーセンサを搭載することによりヒトの瞬目を計測可能な眼鏡型デバイスの開発を目的とする。

眼鏡型デバイスは運転中に装着可能である事から、運転者の眠気検出が可能であり、ヒューマンエラーの抑制に寄与できるものと考えられる。実験はドップラーセンサーにより瞬目を計測すると共に、身体の動きを計測するための加速度センサ、および瞬目信号が正当であることを確認するための EOG を用いて行う。実験結果より、瞬目に関するドップラー周波数は 2Hz 近辺に高い周波数を含むことが確認された。さらに、観測されるデータに頭や体の動きが含まれてしまう場合、PCA を用いてそれらから瞬目信号を分離可能であることを確認できた。

Non-contact measurement of eyeblink by using Doppler sensor

Amir Maleki

Abstract

Many phenomena in the nature exhibit anomalously large temporal fluctuations exceeding what cannot be explained as a consequence of statistically independent random events. Eyeblink is one of the natural parts of human activities which can be used in diverse applications such as Cognitive fields, Human Computer Interfaces etc. For instance, there is a large and growing body of evidence that sequences of psychophysical data fluctuate as $1/f$ noises and many researchers are trying to find what these fluctuations are suggesting us. Considering the fact that eyeblink has been proposed as a marvelous way for detecting driver's and pilot's drowsiness, the importance for eyeblink detection is increasing. There are several ways for eyeblink detection such as the EOG method, Infrared sensors, Cameras, and Doppler sensors. Recently, several types of glasses have been produced, for instance 'Google glass', which is able to detect eyeblink using embedded sensors such as infrared sensors. The objective of this thesis is to develop a glass which can be used to measure human eyeblink through embedding a Doppler sensor inside it, considering to the fact that Doppler sensors have a number of advantages, for instance, long distance detection that is a problem in other methods. This glass can be used during driving and flying in order to detect drowsiness and therefore prevent accidents caused by human errors. Furthermore, it can be deployed for measuring several psychological factors during performing tasks in clinical setups. We designed an

experimental setup in which measurement of the eyeblink was conducted using a Doppler sensor accompanied by an accelerometer for body movement measurements and also an EOG (Electrooculography) recording for verifying detected eyeblink signal by Doppler sensor. From our experimental results, we found that the Doppler frequency related to eyeblink contains a dominant frequency near 2 Hz. Finally, we found that when blinking is accompanied with head and body movements, eyeblink signal is separable by deploying the Principal Component Analysis.

Contents

Figure index	5
Chapter 1 Introduction	8
1.1 Background.....	8
1.2 Motivation	9
1.3 Related works on the eyeblink detection	10
1.3.1 EOG (Electrooculography) method	10
1.3.2 Optical sensors	12
1.3.3 IR (Infrared) sensors	14
1.3.4 Doppler sensors	16
1.4 Application.....	22
1.5 Thesis organization.....	23
Chapter 2 Concept	24
2.1 Doppler Sensor	25
2.2 Accelerometer	26
Chapter 3 Measurement system	27
3.1 EOG recording	28
Chapter 4 Analysis method and results	32
4.1 results when the subject's head and body was steady.....	33
4.2 results when the subject's head and body was not steady	40
Chapter 5 Conclusion and future work	54
Acknowledgment	56
References	57
Publications and conferences	59

Figure index

Figure 1.1 ORBICULARIS OCULI muscle.....	11
Figure 1.2 Infrared proximity sensor built into Google Glass.....	15
Figure 1.3 Blink detection by calculating the peak value.....	16
Figure 1.4 source and motive receiver.....	17
Figure 1.5 motive source and receiver.....	19
Figure 2.1 the concept of the designed glass.....	24
Figure 2.2 Doppler sensor.....	25
Figure 2.3 Accelerometer.....	26
Figure 3.1 Experimental system.....	27
Figure 3.2 EOG recording.....	28
Figure 3.3 MULTI AMPIFIER MA1000-DIGITECS.....	29
Figure 3.4 Experimental setup when the Doppler sensor was fixed to a stand.....	29
Figure 3.5 Experimental setup when the Doppler sensor was attached to a pair of glasses.....	30
Figure 3.6 three different angles for eyeblink detection when the Doppler sensor was mounted on a fixture and head and body were fixed.....	30
Figure 3.7 eyeblink detection when when the Doppler sensor was attached to a pair of glasses.....	31
Figure 4.1 Eyeblink detection flow.....	32

Figure 4.2 Experimental Protocol.....	33
Figure 4.3 a sample of recorded EOG.....	34
Figure 4.4 Spectrum of the recorded EOG.....	34
Figure 4.5 A sample conscious eyeblink detected by Deppler sensor.....	35
Figure 4.6 Spectrum of the Sample conscious eyeblink detected by Deppler sensor.....	35
Figure 4.7 A sample unconscious eyeblink detected by Deppler sensor.....	36
Figure 4.8 Spectrum of the Sample unconscious eyeblink detected by Deppler sensor.....	36
Figure 4.9 Mean of 100 samples of conscious eyeblink.....	37
Figure 4.10 Mean of 100 samples of unconscious eyeblink.....	37
Figure 4.11 Spectrum for mean of 100 samples of conscious eyeblink.....	38
Figure 4.12 Spectrum for mean of 100 samples of unconscious eyeblink.....	38
Figure 4.13 Experimental results when eyeblink was conscious: (a) -45 degree below the eye center, (b) 0 degree and (c) +45 degree above the eye center.....	39
Figure 4.14 Experimental results when eyeblink was unconscious: (a) measured data from -45 degree, below the eye center, (b) 0 degree and (c) +45 degree above the eye center.....	40
Figure 4.15 The arithmetic mean of 100 samples of Doppler signals: (a) when the subject sat in front of the personal computer and performed a routine task and (b) when the subject performed the walking task.....	41
Figure 4.16 The power spectrum of the signals represented in figure 4.14.....	42
Figure 4.17 The accelerometer signals: (a) when the subject sat in front of the personal computer and performed a routine task and (b) when the subject performed the walking task.....	43

Figure 4.18 The Power Spectrum of the signals represented in figure 4.16 (Accelerometer signals).....43

Figure 4.19 First principal components of the signals when the angle between the sensor and the center of eye is 0°: (a) conscious blinking and (b) unconscious blinking.....45

Figure 4.20 The power spectrum of the first to sixth principal components of the signal when the subject sat in front of a personal computer and performed a routine task.....46

Figure 4.21 The power spectrum of the first to sixth principal components of the signal when the subject performed a walking task.....47

Figure 4.22 Reconstructed blinking signal when the subject sat in front of a personal computer and performing a routine task.....48

Figure 4.23 Reconstructed blinking signal when the subject performed a walking task.....49

Figure 4.24 Eyeblink detection procedure when the subject sat in front of a personal computer and performing a routine task.....50

Figure 4.25 Eyeblink detection procedure when the subject performed a walking task.....50

Figure 4.26 The power spectrum of the first to sixth principal components of the signal when the second subject sat in front of a personal computer and performed a routine task.....51

Figure 4.27 The power spectrum of the first to sixth principal components of the signal when the second subject performed a walking task.....52

Figure 4.28 Eyeblink detection procedure when the second subject sat in front of a personal computer and performing a routine task.....53

Figure 4.29 Eyeblink detection procedure when the second subject performed a walking task.....53

Chapter 1 Introduction

1.1 Background

The importance of eyeblink detection has been raised since blinking has been introduced as a complex phenomenon which reflects the influence of higher nervous processes so that different experimental conditions consequences changes in blink patterns. The blink rate decreases significantly while performing visual tasks and this inverse relationship between blink rate and task demands may address mental demands for information processing [1][2]. Recently, development of human-computer interfaces is attracting worldwide attention of researches [3]. In order to measure the blinking activity there are several techniques such as EOG (Electrooculography), image processing, Infrared proximity sensor, Doppler effect sensor, etc. EOG technique is the most precise method but it needs several electrodes to be attached to the skin and it seems somewhat impractical during implementing every day's activities. Image processing methods are noninvasive and detect the blinking patterns by focusing on face recognition. However, in condition such as driving in which the light intensity changes time by time the eyeblink detection may be unsuccessful [3]. One common technique of eyelid movement detection utilizes measurements of infrared (IR) light reflected from the surface of the eye. The performance of current IR sensors, however, is limited by their sensitivity to

ambient infrared noise, by their small field-of-view and by short working distances [4]. Doppler sensors are a non-contact way for measuring eyeblink and it is insensitive to light intensity and it can detect blinking from a considerable long distance. Thus using Doppler sensors has a high potential of becoming a practical way for eyeblink detection. Unfortunately, there are a few researches about the eyeblink detection using Doppler sensor and there is not any concrete method for this type of eyeblink measurement.

1.2 Motivation

Eyeblink may find a verity of applications. As an important example, by detecting the eyeblink rate, the measurement of level of drowsiness in drivers becomes possible and consequently it can drastically reduce the vehicular accidents caused by human failures. Furthermore, eyeblink detection may find applications for measuring several psychological factors, e.g. mental workload, cognitive load, etc. Thus it can be employed for pathological settings and also for improvement of workers efficiency while implementing tasks. The aim of this study is to verify eyeblink detection in several real conditions such as working with computer at office and walking and also develop a method in which the separation of the eyeblink signal from the original signal that is contaminated with head and body movement becomes possible. The speed of a voluntary eyeblink for the closing and opening phases are [52~138 mm/s] and [24~47 mm/s], respectively [5]. Therefore we can estimate that the Doppler frequency of blinking has an approximate range of [1~5.4 Hz]. However, this range can be extended to [1~18 Hz] due to the higher speed of blinking in some human subjects. Our empirical results showed that the head and body movements has the same frequency range as does blinking, therefore detection of eyeblink becomes considerably difficult in real situations

such as performing tasks, walking, etc. Thus conventional low pass filters are almost inefficient. We deployed Principal Component Analysis in order to extract the blinking signals from the mixed raw signals and we observed that there is a high possibility of separating the eyeblink signals.

1.3 Related works on the eyeblink detection

1.3.1 EOG (Electrooculography) method

One of the most precise methods of eyeblink detection is EOG (electrooculography). Eyeblinks are periodic closings and re-openings of the eyelid. The duration of the eyelid closure is used as the criterion to discriminate an eyeblink from an eye closure. An eyeblink closure duration is usually 300 msec and is more typically 200 msec or less. The EOG records changes in the electrical potentials between the cornea and retina as the eyelid movement occurs. The lid closing over the eye causes a difference in the corneal/retinal potential that is evident in the EOG. Therefore, the EOG can be used to detect eyeblinks. However, the measurement of eyeblink can be achieved by placing electrodes on the lower and upper (or vertical) or the left and right (or horizontal) sites of the orbicularis oculi muscle (above and under the right eye) shown in figure 1.1[6].

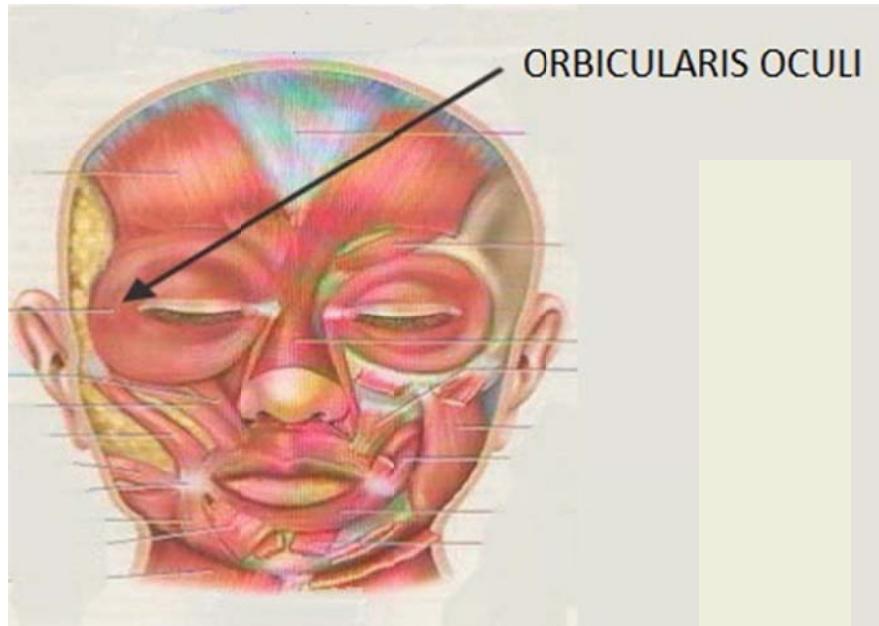


Figure 1.1 ORBICULARIS OCULI muscle, (Anatomy of the Face and Neck, Peter M. Prendergast, 2013).

Usually EOG signals are contaminated with noise including involuntary eyeblink artifacts, EMG, and saccade eye movement. It is proposed that voluntary eyeblink is distinguishable from involuntary eyeblink and the vertical electrode yields better detection of eyeblink, but strayed EMG may be considered as eyeblink by error. One of the methods for eyeblink recognition can be achieved by measuring the average value of eyeblink signal for each individual and when the signal exceed this average value (or any threshold value) the signal is detected. EOG method is reliable but the problem with this method is that it needs some electrodes to be attached to the face skin of the subjects and it is almost impractical for eyeblink detection during performing everyday's tasks [7].

1.3.2 Optical sensors

This method is based on optical tracking of eyelid movements to detect eye blinks. Detection is based on matching SIFT (scale-invariant feature transform) descriptors computed on GPU. First, threshold frame difference inside the eye region locates motion regions. Consequently, these regions are being used to calculate the optical flow. While user blinks, eyelids move up and down and the dominant motion is in vertical direction. This method detects 97% of blinks on their dataset. Most of the false positive detections are the result of gaze lowering and vertical head movements. There are several methods for eyeblink detection, one of them is optical flow estimation. It locates eyes and face position by 3 different classifiers. The algorithm is successful mostly when the head is directly facing the camera. The KLT (Kanade–Lucas–Tomasi) tracker is used to track the detected feature points. This blink detector uses GPU-based optical flow in the face region. The flow within eyes is compensated for the global face movement, normalized and corrected in rotation when eyes are in non-horizontal position. Afterwards dominant orientation of the flow is estimated. The flow data are processed by adaptive threshold to detect eye blinks. Authors report good blink detection rate (more than 90%). However this approach has problems with detecting blinks when eyes are quickly moving up and down. The eyelid movements are estimated by normal flow instead of optical flow. It is the component of optical flow that is orthogonal to the image gradient. Authors claim that the computation of normal flow is more effective than the previous methods. Arai et al. present Gabor filter-based method for blink detection. Gabor filter is a linear filter for extracting contours within the eye. After applying the filter, the distance between detected top and bottom arc in eye region is measured. Different distance indicates closed or opened eye. The problem of arc extraction arises while the person is looking down. Variance map specifies distribution of intensities from the mean value in an image sequence. The intensity of pixels located in eye region changes during the blink, which can be used in detection process. Correlation measures the similarity between actual eye and open eye image. As someone closes eyes during the blink, correlation coefficient decreases. Another blink detection algorithm is based on the fact that the upper and lower part of eye has different distribution of

mean intensities during open eyes and blinks. These intensities cross during the eyelid closing and opening. Liting et al. [8] use a deformable model - Active Shape Model represented by several landmarks as the eye contour shape. Model learns the appearance around each landmark and fits it in the actual frame to obtain new eye shape. Blinks are detected by the distance measurement between upper and lower eyelid. Ayudhaya et al. [9] detect blinks by the eyelid's state detecting (ESD) value calculation. It increases the threshold until the resulting image has at least one black pixel after applying median blur filtering. This threshold value (ESD) differs while user blinks.

Here we will introduce briefly two proposed methods based on histogram backprojection and the Inner movement detection based on KLT feature tracker.

1.3.2.1 Histogram Backprojection

Histogram backprojection creates a probability map over the image. In other words backprojection determines how well the pixels from the image fit the distribution of a given histogram. Higher value in a backprojected image denotes more likely location of the given object. High percentage of skin color pixels within the eye region represents closed eyes and otherwise eyes are considered opened.

1.3.2.2 Inner Movement Detection

Optical flow is usually used in this method. *Optical flow* is the relation of the motion field:

The 2D projection of the physical movement of points relative to the observer to 2D displacement of pixel patches on the image plane. One of the most common methods called KLT tracker selects features suitable for tracking with high intensity changes in both directions.

If a user blinks, the mean displacement of feature points within the eye region should be greater than the displacement of the rest of the points within the face area.

The first step consists of localizing a user's face and eyes using *Haar Cascade Classifier* on grayscale image. Then random KLT features within the eye and nose regions are initialized and classified as left ocular, right ocular or non-ocular. These features are being tracked by KLT tracker. Tracking is reinitialized in regular intervals or in case of loss of many feature points. After that the average displacement is computed separately for three groups of points. Finally, the difference between the left or right ocular and non-ocular movement displacements is computed. If this difference exceeds a threshold value, a movement within the eye region is anticipated [10].

1.3.3 IR (Infrared) sensors

Another common method of eyeblink recording utilizes infrared (IR) photoelectric sensors. This approach measures IR light reflected from the surface of the eye. A typical IR eyeblink measurement device consists of an IR light emitting diode (LED), which illuminates the eye surface, paired with an IR photodiode that detects IR light reflected back from the eye [11].

An ideal IR eyeblink detector should have several important properties. To detect the full range of eyelid movement, the IR LED should completely illuminate the surface of the fully opened eye, and in addition, the field-of-view of the IR photodiode should encompass the whole eye area. Some currently used detectors rely on commercial proximity sensors that not only must be positioned close to the eye but also emit a narrow IR beam resulting in incomplete coverage of the full range of eyelid motion. Google glass implements an infrared proximity sensor facing the users' eye that can be used for blink detection shown in Figure 1.2.



Figure 1.2 Infrared proximity sensor built into Google Glass (Ishimaru et al., 2014).

1.3.3.1 Blink detection

Blinks are detected based on the raw infrared proximity sensor signal. A sliding window is moved on the sensor data stream and monitored whether the center point of each window is a peak or not according to the following definition. The distance from one sensor value of the center point in the window (p_5 in Figure 1.3) to the average value of other points (p_1, p_2, p_3, p_7, p_8 and p_9) is calculated. The preceding and subsequent points of the center (p_4 and p_6) are excluded from the average calculation because their sensor values are often affected by the center point. If the distance is larger than a threshold ranging from 3.0 - 7.0, the center point is defined as a blink. Because the shape of the face and eye location vary, the best threshold for the peak detection varies for each user. IR sensors are noninvasive but their field-of-view and working distance are small and short respectively.

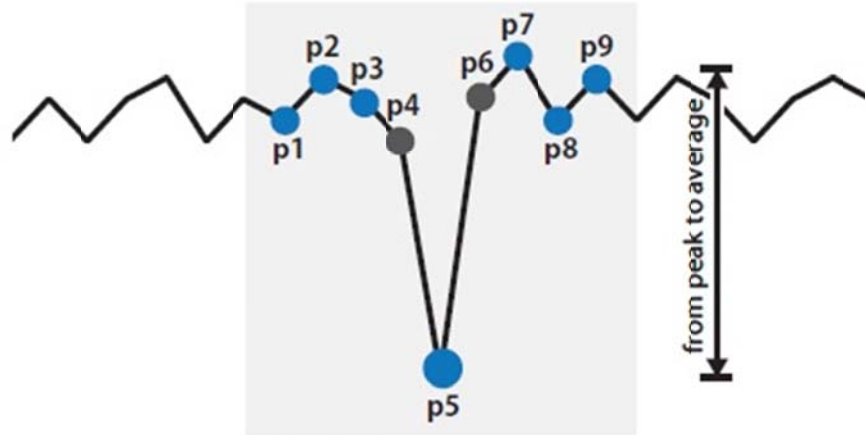


Figure 1.3 Blink detection by calculating the peak value (Ishimaru et al., 2014).

1.3.4 Doppler sensors

Electromagnetic waves have been utilized for the detection of eye blinking. When a moving object is illuminated by a continuous wave, it generates a Doppler shift on the frequency of the return signal.

1.3.4.1 Doppler Effect

The Doppler Effect is the change in the observed frequency of a source due to the relative motion between the source and the receiver. The relative motion that affects the observed frequency is only the motion in the Line-Of-Sight (LOS) between the source and the receiver.

If a source is stationary, as the one shown in figure 1.4, it will emit sound waves that propagate out from the source as shown below. As the receiver moves towards the source, it will detect the sound coming from the source but each successive sound wave will be detected earlier than it would have if the receiver were stationary, due to the motion of the receiver in the LOS. Thus the frequency that each successive wave front would be detected would be changed by this relative motion where:

$$\Delta f = \frac{V_r}{\lambda_0} \quad \text{Eq 1.1}$$

λ_0 is the original wavelength of the source

Δf is the change in the observed frequency

V_r is the velocity of the receiver in the LOS

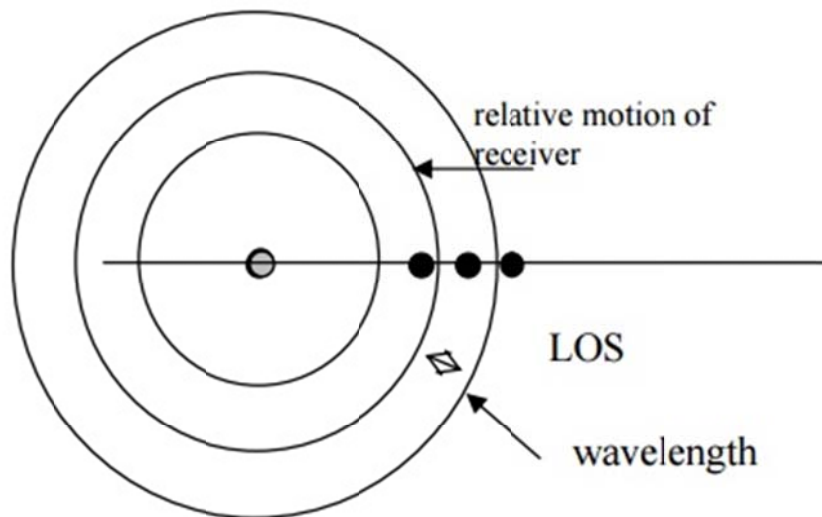


Figure 1.4 source and motive receiver.

Since the original frequency of the source can be expressed in terms of the wavelength where $f_0 = c/\lambda_0$, the observed frequency becomes:

$$f' = f_0 + \Delta f \quad \text{Eq 1.2}$$

$$f' = \frac{c}{\lambda_0} + \frac{V_r}{\lambda_0} \quad \text{Eq 1.3}$$

$$f' = f_0 \left(\frac{c + V_r}{\lambda_0} \right) \quad \text{Eq 1.4}$$

Note that this equation only works if the relative velocity of the receiver, V_r is towards the source. If the motion is away from the source, the relative velocity would be in the opposite direction and the equation would become:

$$f' = f_0 \left(\frac{c - V_r}{\lambda_0} \right) \quad \text{Eq 1.5}$$

The two equations are usually combined and expressed as:

$$f' = f_0 \left(\frac{c \pm V_r}{\lambda_0} \right) \quad \text{Eq 1.6}$$

If the source is moving towards the receiver, the effect is slightly different. The spacing between the successive wave fronts would be less as seen in the figure 1.5. This would be expressed as:

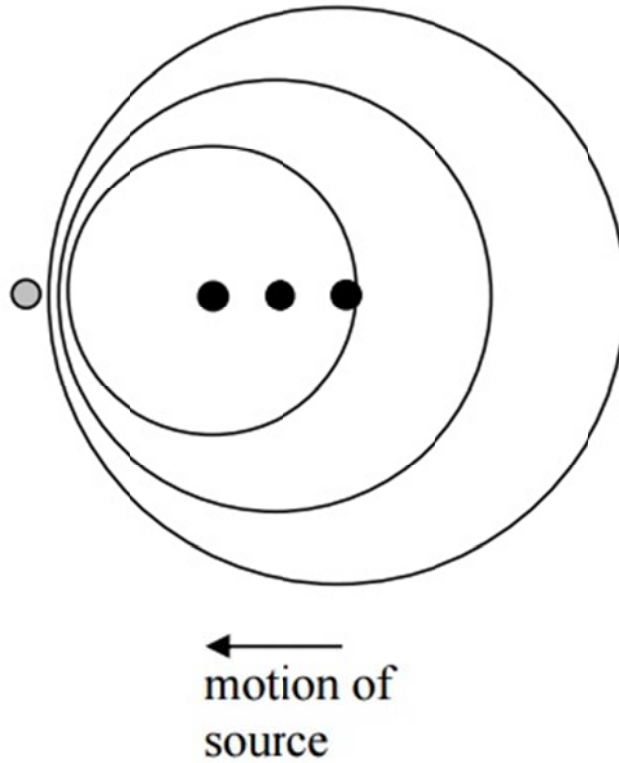


Figure 1.5 motive source and receiver.

$$\Delta \lambda = \frac{V_s}{f_0} \quad \text{Eq 1.7}$$

V_s is the relative velocity of the source

To calculate the observed frequency:

$$f' = \left(\frac{c}{\lambda_0 + \Delta \lambda} \right) \quad \text{Eq 1.8}$$

$$f' = f_0 \left(\frac{c}{c - V_s} \right) \quad \text{Eq 1.9}$$

Note that this is only when the source is moving towards the receiver. If the source is moving away, the equation would be changed to:

$$f' = f_0 \left(\frac{c}{c + V_s} \right) \quad Eq\ 1.10$$

When combined with the previous result, the equation would be expressed as:

$$f' = f_0 \left(\frac{c}{c \mp V_s} \right) \quad Eq\ 1.11$$

Notice that this time, the plus/minus symbol is inverted because the sign on top is to be used for relative motion of the source towards the receiver.

By combining the previous results, we can derive one equation to use as the Doppler Equation.

This is usually expressed as:

$$f' = f_0 \left(\frac{c \pm V_r}{c \mp V_s} \right) \quad Eq\ 1.12$$

It must be noticed that the quantities for the velocity of the receiver, V_r , and the velocity of the source, V_s , are only the magnitudes of the relative velocities in (or along) the LOS. In other words, the component of the velocity of the source and the receiver, that are perpendicular to the LOS do not change the received frequency. Secondly, the top sign in the numerator and the denominator are the sign convention to be used when the relative velocities are towards the other. If the source were moving towards the receiver, the sign to use in the denominator would be the minus sign. If the source were moving away from the receiver, the sign to use would be the plus sign.

1.3.4.2 Eyeblink measurement using Doppler Effect

By the time of writing this thesis there are only two related works that explain eyeblink detection using Doppler effect:

One work was conducted by Kamil et al. in 2012. The research was carried out in order to measure the level of drowsiness in drivers. They deployed a multiple receiver microwave Doppler radar. The sensor was consisted of a synthesized signal source with the output frequency of 9 GHz. The system implemented a single side band SSB modulation and a quadrature modulator structure. The modulation frequency was 1 KHz and the antenna was a 16-element, 4x4array. The receiver was consisted of 8 channels that integrated IQ mixers [3].

In order to find the signal's characteristics they implemented several methods and they reported that:

- Through frequency analysis, FFT, of the recorded eyeblink signal, the frequency related to blinking is completely covered by the spectrum of general head movement signal.
- Implementing Continuous Wavelet Transform (CWT) they reached the same results as FFT.
- They could not find any useful information in signal phase extraction.
- Finally they selected time domain analysis in order to reach the eyeblink signal and introduced a separated wave form for eyeblink detected by Doppler sensor.

As the signal detection procedure after passing the measured signal and signal denoising procedure using multilevel discrete wavelet decomposition, they achieved a signal containing several sinusoidal waveforms. In the next step, they calculated the envelope of the represented signal by using a simple rectangular filter. Finally, they determined a threshold and when the amplitude of the envelope exceeded the threshold they considered the signal as a blink. Unfortunately, they didn't provide detailed information for their experimental method and also the frequency characteristics of the eyeblink signal remains undetermined.

Another study aimed to detect eyeblink using Doppler sensor was conducted by Youngwook Kim in 2015. He performed several measurements with/without the noise caused by human movement when the sensor was placed near the eyes. Then he analyzed the Doppler signal in the joint time–frequency domain and suggested that the Doppler frequency produced by eye blinking was approximately 115 Hz. Furthermore, he proposed that unconscious and conscious eye blinking exhibited different Doppler characteristics and deployed Principal Component Analysis In order to classify these characteristics. Then he introduced a method in which conscious and unconscious eyeblink can be distinguished by multiplying truncated eigenvectors with an image of eye blinking [12].

Kim implemented PCA method as an image processing method of target recognition for distinguishing the conscious from unconscious blinking and also noise. He represented the sorted eigenvalues, in which two eigenvalues contain more than 97% of the total energy and the reconstructed two-dimensional images from the one dimensional eigenvectors that corresponded to the highest eigenvalues. He claimed that the first eigenvector was similar to the image of conscious eye blinking, and the second eigenvector was analogous to that of the unconscious eye blinking.

1.4 Application

Eyeblink detection may find many applications in a wide variety of the fields. For instance investigation of eye-blinking activity can have applications in the detection of the unconsciousness of pilots and the drowsiness of drivers. One study was conducted in 2013 by Genis et al. in order to investigate connection between changes in blinking and changes in a driving- task difficulty. They implemented a camera located inside a car for blink detection. They reported that changes in task difficulty follow fluctuation in eyeblink frequency [14].

Another study was performed in 1998 in order to measure the Physiological workload reactions to increasing levels of task difficulty. They measured blink intervals when changing a pilot-task difficulty and they observed that eyeblink interval fluctuates with task difficulty level and this feature can be used for measuring the mental workload level allocated to each task. Furthermore, eyeblink can be used as a simple communication (yes/no) for soldiers in the battlefield and patients with spiral-cord injuries, where normal verbal communication is not possible. In addition, eye blinking can serve as a communication methodology such as human input into a computer. For example, eye blinking has also been studied for the development of a head set type computer mouse designed for the disabled [15].

1.5 Thesis organization

✓ **Chapter 1: Introduction**

We discuss about the background, application, motivation and related works on eyeblink detection in this chapter.

✓ **Chapter 2: Concept**

In this chapter we introduce our concept about making a glass for eyeblink detection.

✓ **Chapter 3: Measurement system**

We introduce the measurement method and system for this study and also we give detail information about experimental items.

✓ **Chapter 4: Analysis method and results**

In this chapter we represent our analysis method that is based on PCA method. We also show our experimental results in this chapter.

✓ **Chapter 5: Conclusion**

The conclusion of this study has been discussed in this chapter. We also have an overlook on the future part of this study.

Chapter 2 Concept

Developing a glass which is able to detect eyeblink in human subjects is the major objective of this thesis. This glass can measure the eyeblink in diverse conditions. It can be used to measure the drowsiness state in drivers and pilots and therefore prevent accidents caused by human errors. We deployed a Doppler sensor, attached to a pair of glasses for eyeblink detection and also we used an accelerometer for head and body movement measurement. This Accelerometer plays a part in the analysis and measurements. Figure 2.1 depicts the glass.

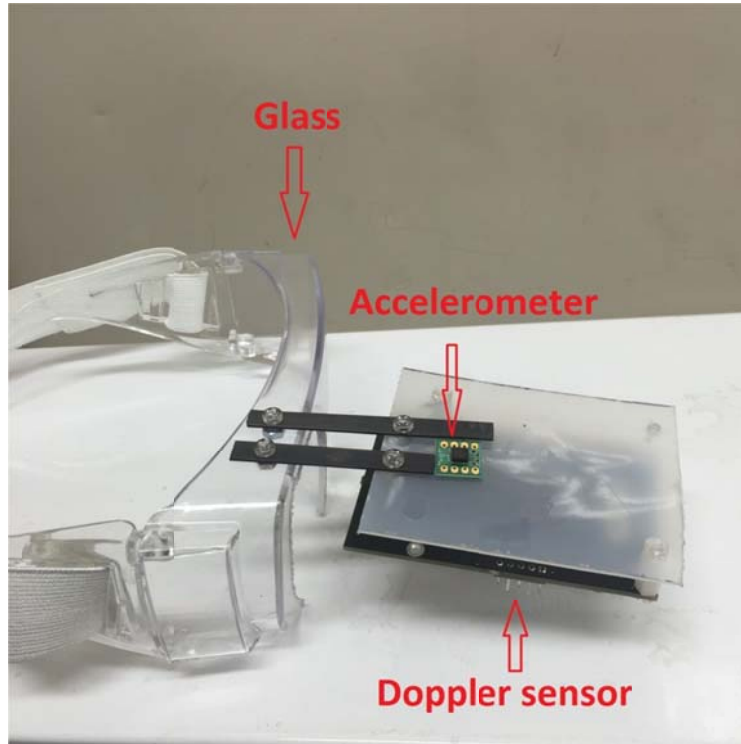


Figure 2.1 the concept of the designed glass.

The following we will introduce each part of the glass. Where, the glass itself is a plastic eye protection glass without any metal part which may cause some disturbance in the

electromagnetic waves produced by the Doppler sensor and therefore consequences faults in the experimental measurements.

2.1 Doppler Sensor

Figure 2.2 shows the Doppler sensor employed in our experiment. The sensor is a low-power Pulsed Doppler Radar (PDR) and has a detection range up to 10 m. the center frequency is 5.8 GHz which corresponds to a wavelength of about 5.2 cm. it has an on-board dipole antenna with a 60 degree conical coverage pattern. The output is a Coherent quadrature output (I & Q) and it responds to radial velocities between 2.6 cm/s and 2.6 m/s, manufactured by Samraksh Co. In this study we calculated the amplitude of the Doppler sensor's quadrature output, i.e. $\sqrt{I^2 + Q^2}$ across all the study.



Figure 2.2 Doppler sensor.

The relation between radial velocity and Doppler frequency is:

$$F_d = \frac{2V_r}{\lambda} \quad \text{Eq 2.1}$$

Where F_d is the Doppler frequency, V_r is the radial component of the target's velocity, and λ is the wavelength at the center frequency.

2.2 Accelerometer

The Accelerometer is ADXL335 shown in figure 2.3. The sensor is a small, thin, low power, complete 3-axis accelerometer with signal conditioned voltage outputs. It measures acceleration with a minimum full-scale range of ± 3 g. It can measure the static acceleration of gravity in tilt-sensing applications, as well as dynamic acceleration resulting from motion, shock, or vibration. The sensitivity of sensor is 300 mV/g. we calculated the amplitude of these axes ($\sqrt{(x^2 + y^2 + z^2)}$) for this study.



Figure 2.3 Accelerometer.

Chapter 3 Measurement system

Figure 3.1 depicts the experimental system. This system consists of a Doppler sensor for eyeblink detection, and accelerometer for head and body measurement and an EOG recording conducted by placing three electrodes placed on the subjects face and using a multi amplifier.

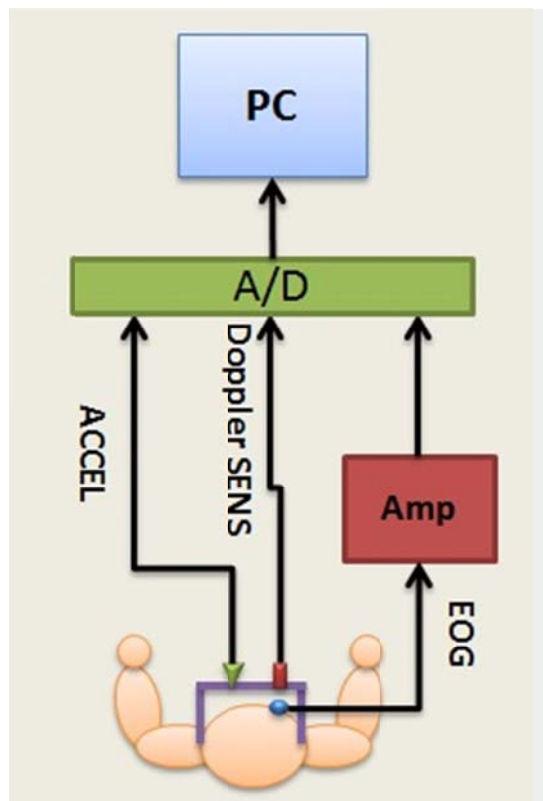


Figure 3.1 Experimental system.

All recordings took place using a personal computer after converting the analogue signals to digital by the A/D board.

3.1 EOG recording

The EOG recording for the eyeblink took place by placing two electrodes to the lower and upper sites of the orbicularis oculi muscle (above and under the right eye) and one electrode placed over the forehead as the ground electrode, represented in figure 3.2. In order to verify the blinking signals collected by the Doppler sensor the EOG were recorded using a MULTI AMPIFIER MA1000-DIGITECS. As we can see the positive and negative electrodes was paced on the upper and lower sites of the orbicularis oculi, respectively. Before attaching the electrodes the surface of the skin was cleaned carefully for reducing the skin resistance and better measurement of the EOG. The setting for the Multi amplifier was: TC = 0.3 Sec, HFF = 100 Hz, Sensitivity = 500 μ V, the reference setting was standard.

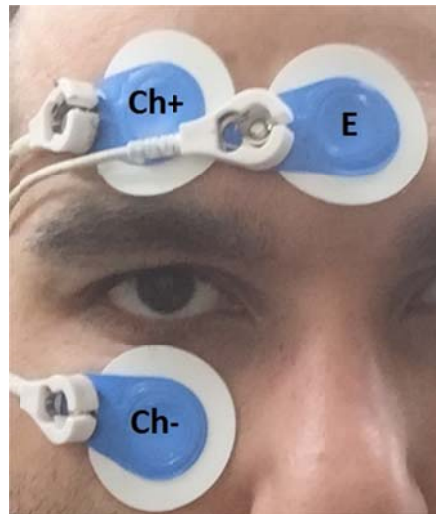


Figure 3.2 EOG recording.

Figure 3.3 shows the MULTI AMPLIFIER MA1000-DIGITECS.



Figure 3.3 MULTI AMPLIFIER MA1000-DIGITECS.

Doppler and Accelerometer sensors recordings were carried out through a sample frequency of 1000 Hz by using an AD board (TRM-7100) manufactured by Interface.

Our experiment was conducted in two parts:

- 1- When the Doppler sensor was fixed to a stand, shown in figure 3.4.
- 2- When the Doppler sensor was attached to a pair of glasses, depicted in figure3.5.

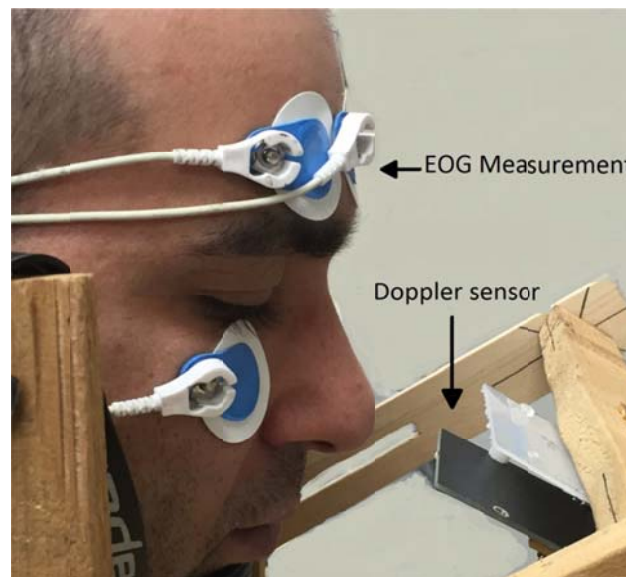


Figure 3.4 Experimental setup when the Doppler sensor was fixed to a stand.



Figure 3.5 Experimental setup when the Doppler sensor was attached to a pair of glasses.

In part 1, the Doppler signal produced by eyeblink was measured from three different angles: -45 degree (under the eye), 0 degree (horizontal to the eye or at the same level with the eye) and +45 degree (above the eye), shown in figure 3.6. The distance between the eye and Doppler sensor was 5 cm.

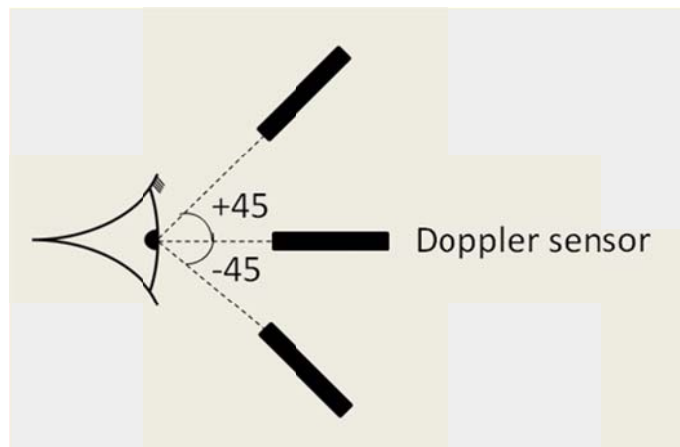


Figure 3.6 three different angles for eyeblink detection when the Doppler sensor was mounted on a fixture and head and body were fixed.

In part 2, the Doppler Sensor was attached to the glass and the distance between the eye and Doppler sensor was 5 cm. In this part the angle between the eye and Doppler sensor was 0° across all measurements, depicted in figure 3.7.

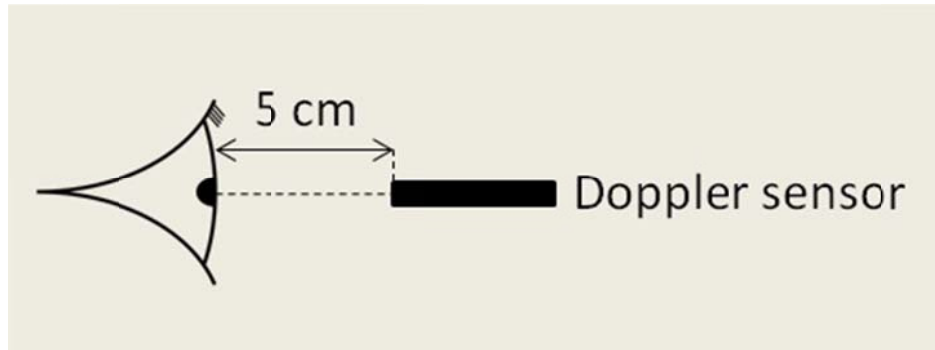


Figure 3.7 eyeblink detection when when the Doppler sensor was attached to a pair of glasses.

Then the measurement was conducted in two conditions:

- 1- When subjects sat in front of a personal computer and performed a routine task.
- 2- When subjects performed a walking task.

Chapter 4 Analysis method and results

As the procedure of the eyeblink detection, first, we recorded and verified eyeblink using Doppler sensor and EOG when the head and body were steady. Then we analyzed obtained data in order to define the dominant frequency associated with each subject. Next, we measured the eyeblink signal recorded by Doppler signal during performing two tasks in which the head and body were not steady and the subjects could able to move their heads and bodies arbitrary. We also recorded the head and body movement using the accelerometer at this stage. After that, we applied PCA method to the collected Doppler signals, contaminated with the head and body movement, in order to separate the eyeblink signal from them. Finally, we selected the principal components which had the same dominant frequency and calculated the mean of them as the reconstructed eyeblink signal. The eyeblink detection was performed by defining a threshold value. Figure 4.1 depicts the eyeblink detection flow. The analysis was conducted using MATLAB software.

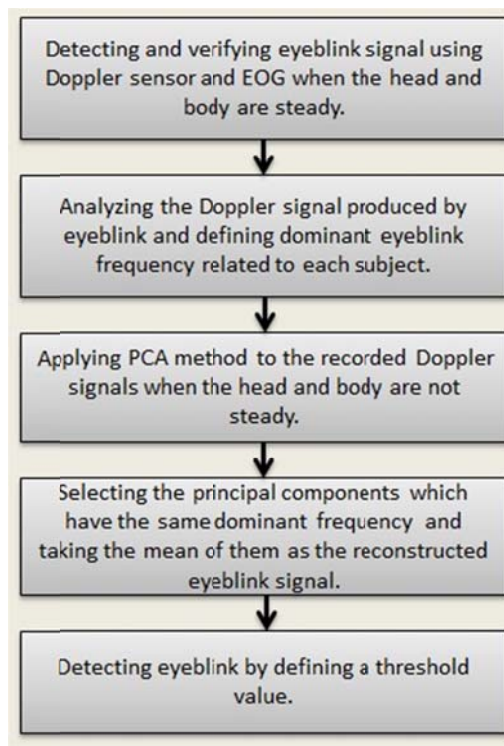


Figure 4.1 Eyeblink detection flow.

4.1 results when the subject's head and body was steady

In this part we measured both EOG and Doppler signal when the subjects placed their head on a fixture. The EOG signal was passed through a low pass filter. In fact we have recorded the EOG signals in order to confirm each eyeblink' detection using Doppler signal. As the procedure for signal detection first we calculated the global maximum of the EOG signal for each measurement and then we cropped half a second of recorded Doppler signal before and after the global maximum of the EOG, this is shown in figure 4.2. In this figure the blue signal represents the EOG recording and the red signal represents the original eyeblink signal recorded by the Doppler sensor.

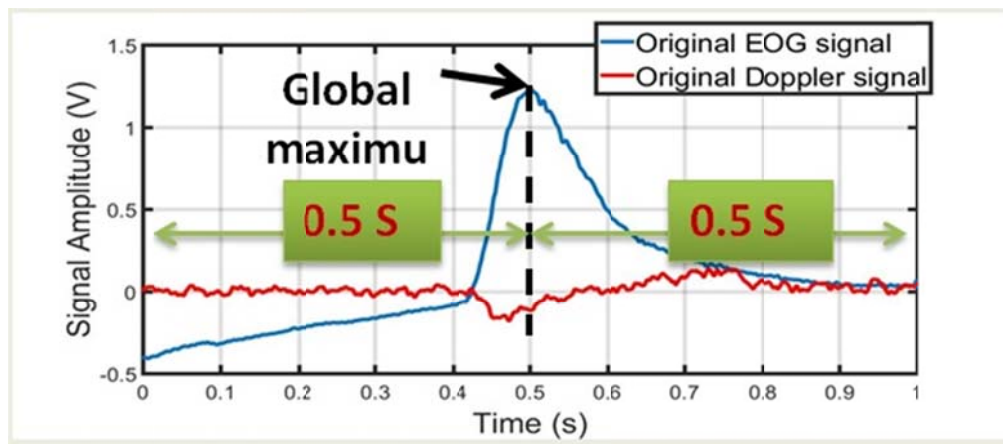


Figure 4.2 Experimental Protocol.

Following the fact that the sampling frequency was 1 KHz therefore we had 1000 data-points for each eyeblink sample. We collected 100 samples for each measurement for both conscious and unconscious blinking. Figure 4.3 represents a sample of recording EOG and figure 4.4 shows the corresponding frequency spectrum.

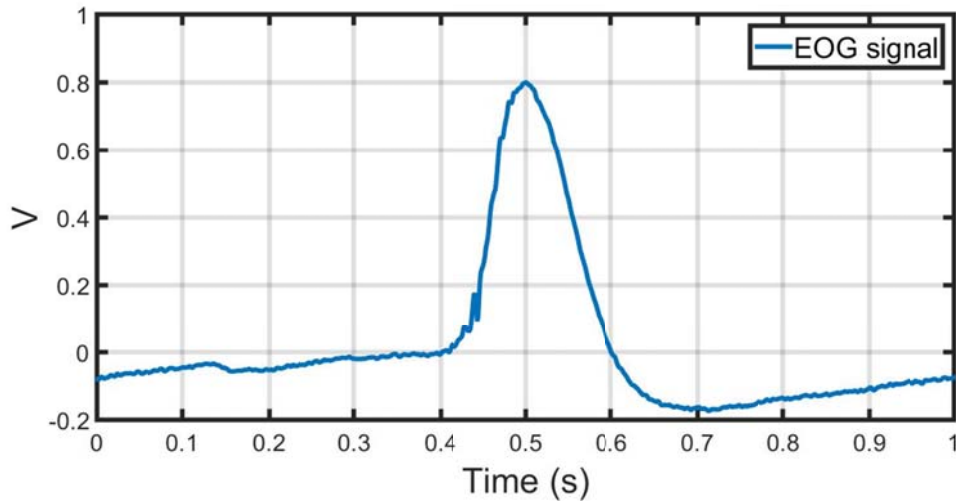


Figure 4.3 a sample of recorded EOG.

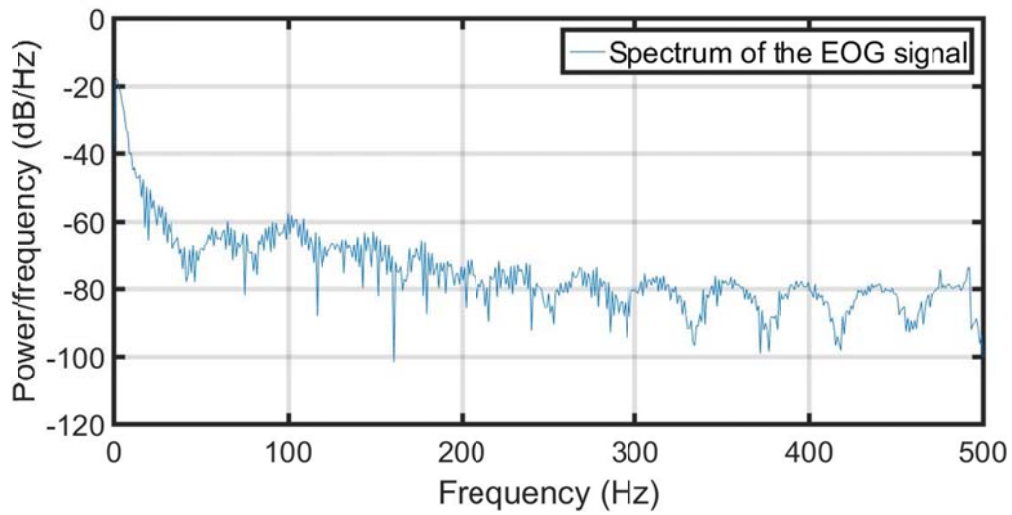


Figure 4.4 Spectrum of the recorded EOG.

From the Power spectrum of the EOG signal we can see that most of the power of the signal is located in the frequencies up to 10 Hz. Figure 4.5 and figure 4.6 show one sample of the original recorded conscious eyeblink and its power spectrum respectively when the angle between the eye and Doppler sensor was 0° . As we can see most of the powerful frequencies are under 10 Hz.

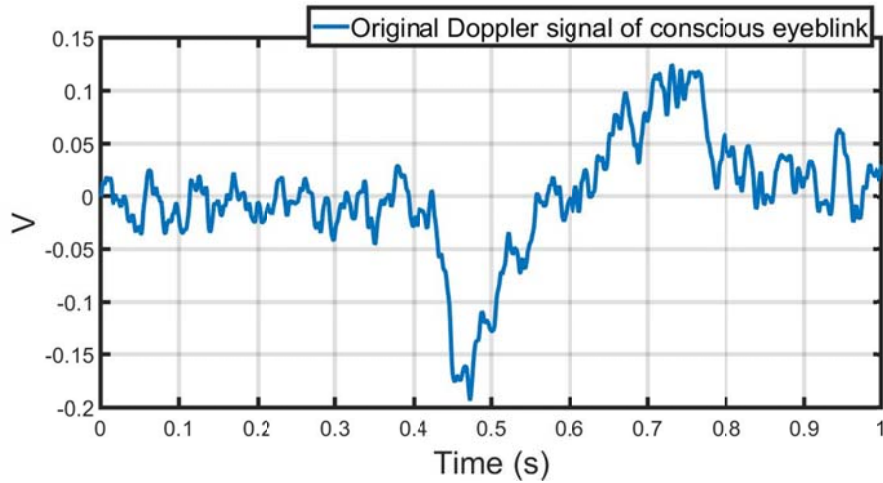


Figure 4.5 A sample conscious eyeblink detected by Doppler sensor.

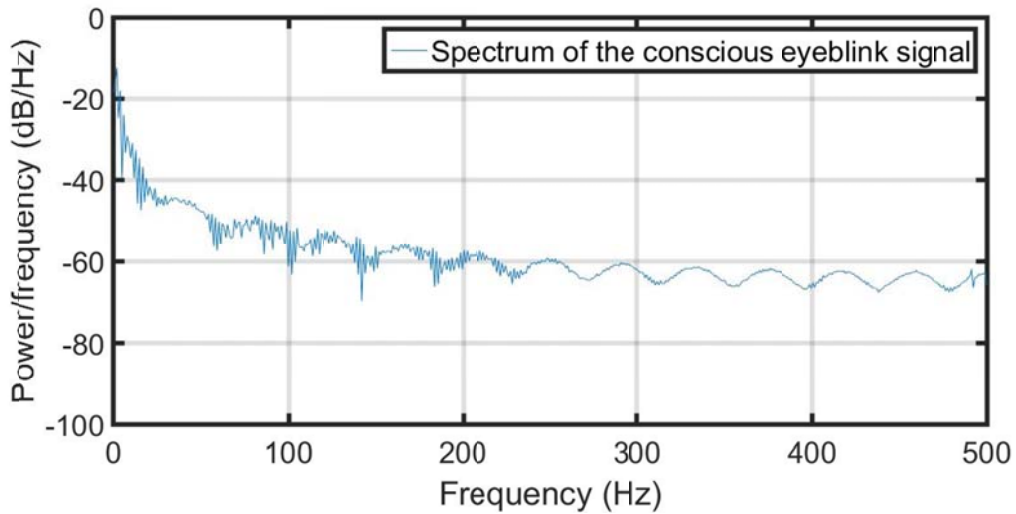


Figure 4.6 Spectrum of the Sample conscious eyeblink detected by Doppler sensor.

Figure 4.7 and figure 4.8 depicts the case for the original recorded conscious eyeblink and its power spectrum respectively when the angle between the eye and Doppler sensor was 0° . As we can see most of the powerful frequencies are under 10 Hz.

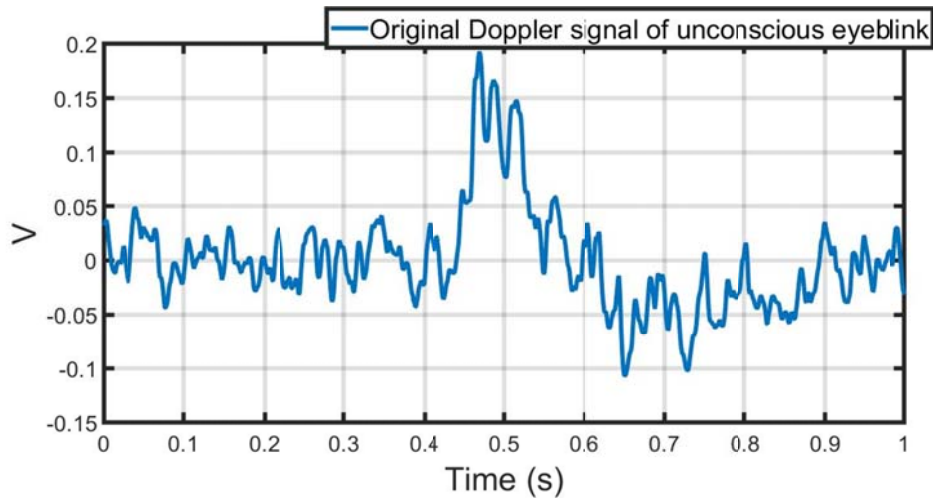


Figure 4.7 A sample unconscious eyeblink detected by Doppler sensor.

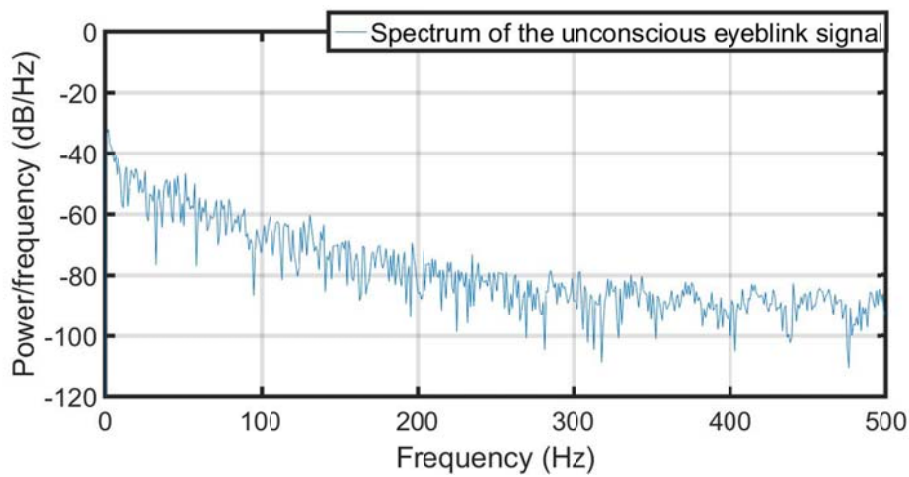


Figure 4.8 Spectrum of the Sample unconscious eyeblink detected by Doppler sensor.

As a result we can see that conscious and unconscious eyeblink have different waveforms and it can be greatly used in order to distinguish between conscious and unconscious eyeblink. To better understanding the conscious and unconscious eyeblink wave form and their frequency characteristics we calculated the arithmetic mean of 100 samples for each measurement:

$$\bar{x} = \frac{1}{100} \sum_{i=1}^{100} x_i \quad \text{Eq 4.1}$$

Figure 4.9 to figure 4.10 represent the results for both conscious and unconscious blinking when the angle between the eye and Doppler sensor is 0°.

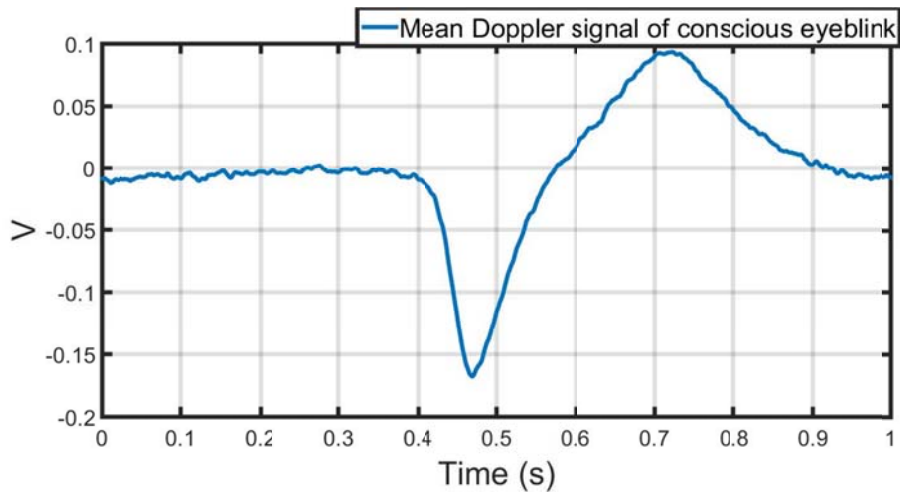


Figure 4.9 Mean of 100 samples of conscious eyeblink.

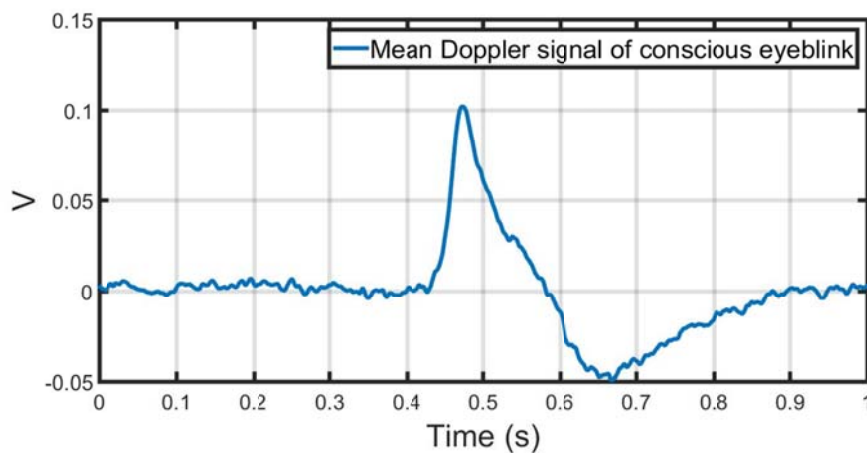


Figure 4.10 Mean of 100 samples of unconscious eyeblink.

Figures 4.11 and Figure 4.12 represents the power spectrum of the represented signals in figure 4.8 and figure 4.9. For better analyzing the frequency features of the eyeblink we have selected those frequencies less than 20 Hz.

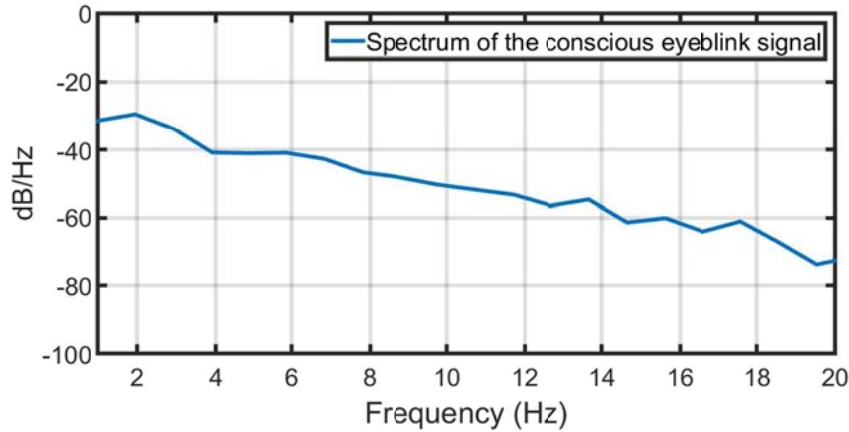


Figure 4.11 Spectrum for mean of 100 samples of conscious eyeblink.

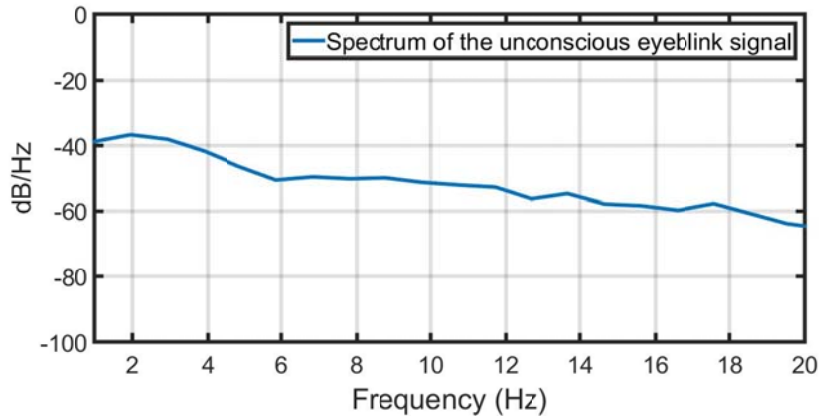


Figure 4.12 Spectrum for mean of 100 samples of unconscious eyeblink.

As a result we can see that the dominant frequencies for both conscious and unconscious blinking are near 2 Hz. However this frequency depends only to the blinking speed of subjects and may vary for each individual. As we introduced in the previous chapter that the average speed of eyelid has been suggested [52~138 mm/s] and [24~47 mm/s] for closing and opening phase, respectively. Thus as we expected the obtained frequency is within the proposed frequency range associated with eyelid speed [1~5.4 Hz].

Figure 4.13 and Figure 4.14 show the measured Doppler signal produced by eyeblink from three different angles; -45° , 0° , 45° ; for both conscious and unconscious eyeblink, respectively.

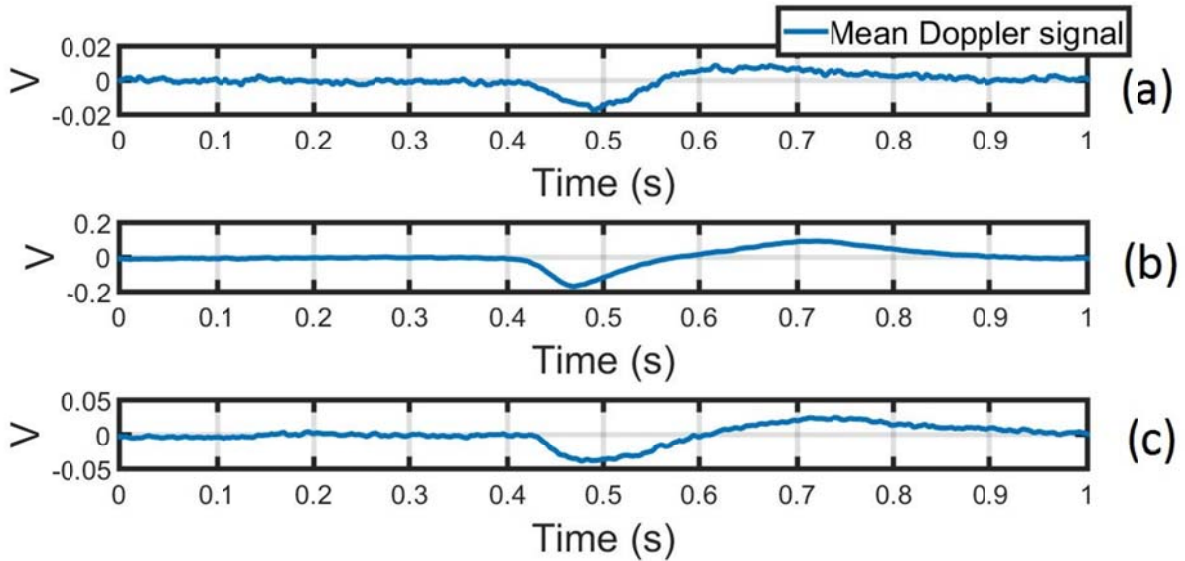


Figure 4.13 Experimental results when eyeblink was conscious: (a) -45° degree below the eye center, (b) 0° degree and (c) $+45^\circ$ degree above the eye center.

As we can see in this figure, obviously, the eyeblink is well detectable from a wide detection angle between -45° to $+45^\circ$. This means that eyeblink detection is practical in a condition that the sensor is fixed and the head is moving upward and downward. However, the best detectable angle is 0° because the radial velocity of the eyelid has the maximum value at this position.

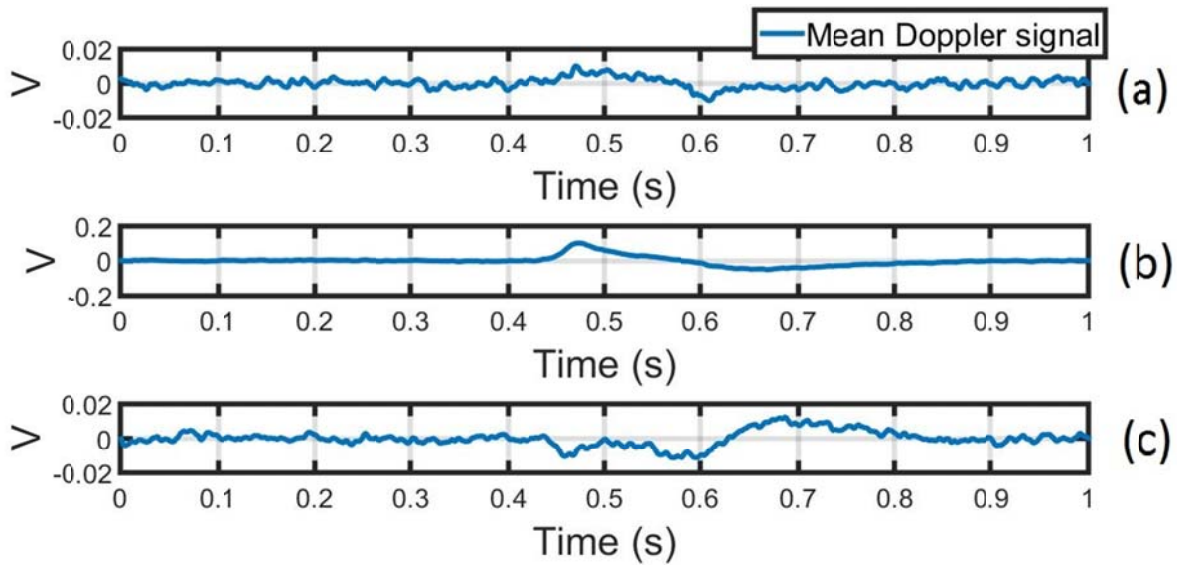


Figure 4.14 Experimental results when eyeblink was unconscious: (a) measured data from -45 degree, below the eye center, (b) 0 degree and (c) +45 degree above the eye center.

In this figure we also see that the eyeblink is well detectable from a wide angle range between -45° to $+45^\circ$ and the best detectable angle is 0° . But we observed that the conscious and unconscious blinking have different waveforms and also the detected signal of conscious blinking is stronger than that of unconscious blinking due to the fact that in the conscious blinking the eyelid movement is accompanied with the muscle movements around the eye.

4.2 results when the subject's head and body was not steady

In this part we measured the eyeblink signal for two conditions:

1. When the subject sat in front of a personal computer and performed an everyday task, in this case the subject was able to move his head arbitrary.

2. When the subject performed a walking task.

In this part due to the more powerful signal in conscious blinking we only study the conscious eyeblink. Figure 4.15 and 4.16 show the arithmetic mean of the 100 collected samples for both conditions.

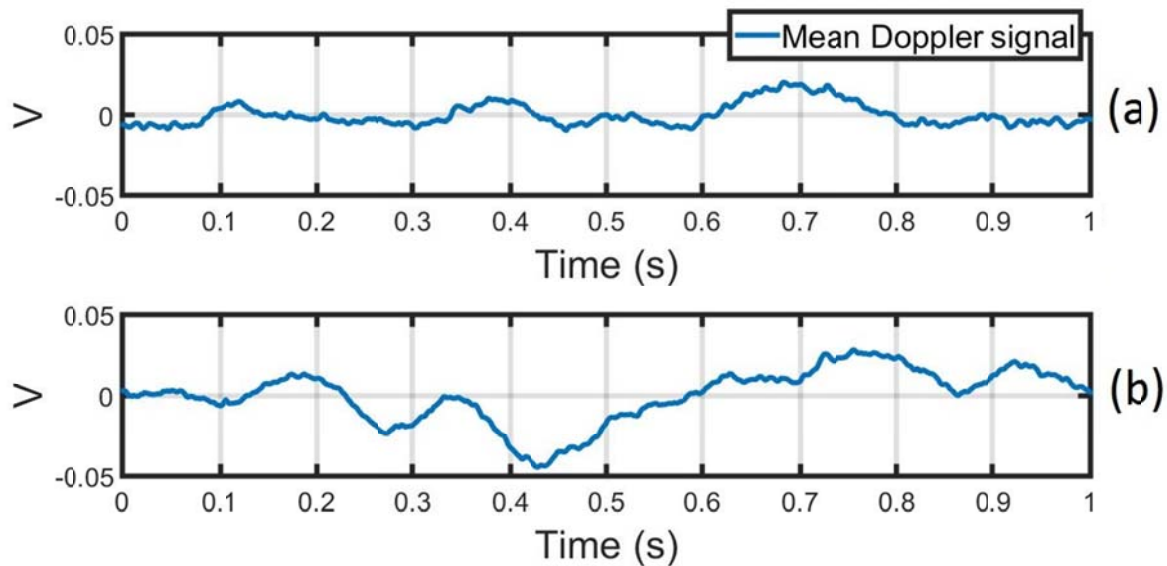


Figure 4.15 The arithmetic mean of 100 samples of Doppler signals: (a) when the subject sat in front of the personal computer and performed a routine task and (b) when the subject performed the walking task.

As we can see the measured signals by the Doppler sensor are completely distorted by the head and body movement and we need to find a way to separate eyeblink signal from the distorted signal. There are several proposed ways for signal separation. One of them is to pass the signal through a low pass or band pass filter, but due to the fact that eyeblink and head and body movements have similar frequency components and as it has been reported in the previous works by some authors, using common filters seems almost hopeless. As another method for signal separation, ICA (Independent Component Analysis) is widely used for signal separation purposes. We examined ICA method in our study, but due to the inefficient impact of ICA on the signal separation procedure and therefore poor results, we tried to find another method and finally we selected PCA method.

Before applying PCA method, in order to study frequency characteristics we calculated the power spectrum of the recorded signals. Figure 4.16 depict the results.

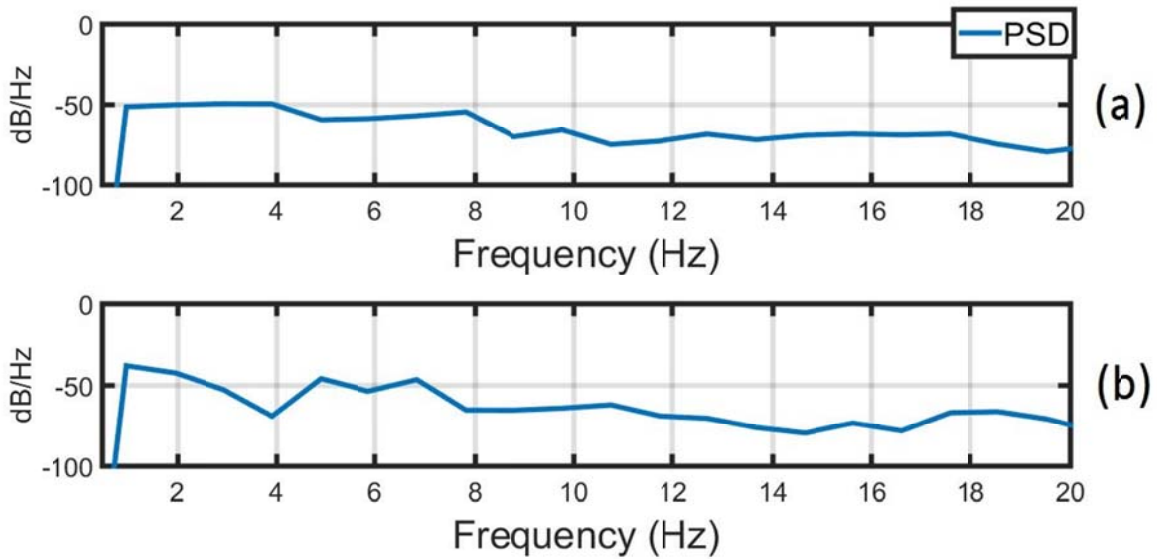


Figure 4.16 The power spectrum of the signals represented in figure 4.14.

We can see that in figure 4.16 (a), frequencies from 2 to 4 Hz and in figure 4.16(b), except frequencies near 2 Hz the signal has most of its power in frequencies between 5 to 7 Hz. In order to better understanding this feature we also measured the body movement using the accelerometer. Figure 4.17 shows the recorded head and body movements using the Accelerometer and figure 4.18 represents its power spectrum.

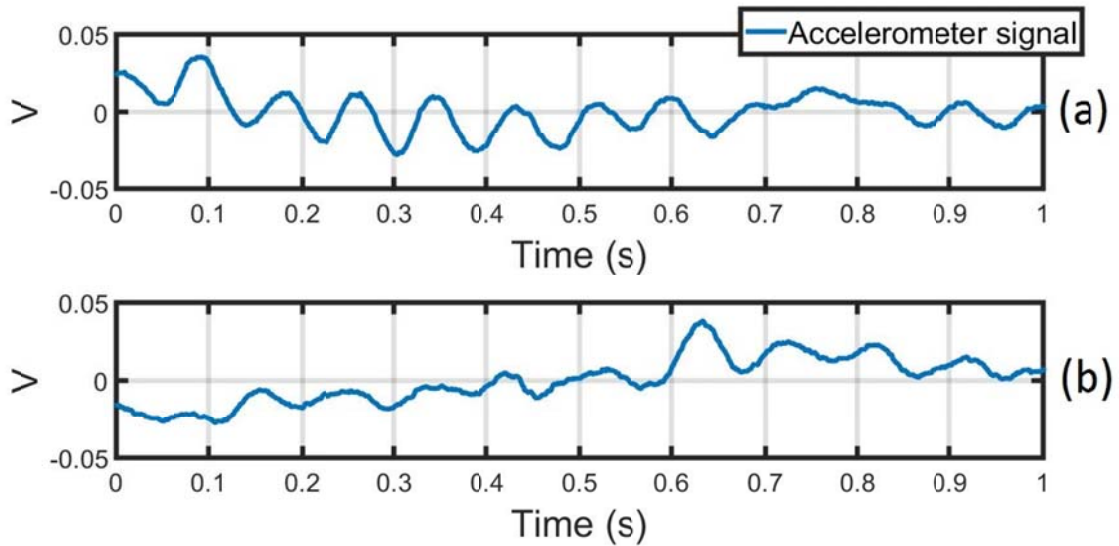


Figure 4.17 The accelerometer signals: (a) when the subject sat in front of the personal computer and performed a routine task and (b) when the subject performed the walking task.

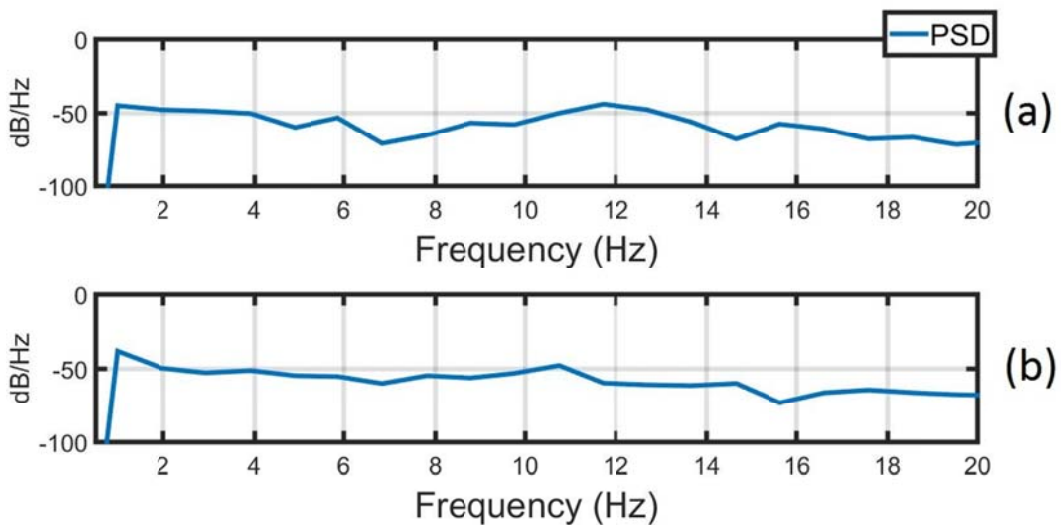


Figure 4.18 The Power Spectrum of the signals represented in figure 4.16 (Accelerometer signals).

From the frequency characteristics of the head and body movements we can see that those frequencies between 10 to 13 Hz are the dominant frequency for this particular subject. Now that we know which frequencies contain the most powerful part of the signal, in the next section we have tried to separate the eyeblink signal from the original measured signal using PCA method.

4.3 Applying PCA for signal separation

In this section in order to extract the principal components of the original signals we implemented the Principal Component Analysis (PCA) [13]. In the previous parts each original signal was divided into 100 datasets of 1000 point length (or one seconds), thus we obtained 100 samples of eyeblink signals for each measurement. Then we arranged these samples into matrices so that the size of each matrix was 100×1000. Then we calculated the PCA of each matrix.

$$X = \begin{pmatrix} X_{1,1} & \cdots & X_{1,1000} \\ \vdots & \ddots & \vdots \\ X_{100,1} & \cdots & X_{100,1000} \end{pmatrix} \quad Eq 4.1$$

So that:

$$X = U \times S \times V^T \quad Eq 4.2$$

In which:

U is the leftsingular vectors

V is the rightsingular vectors

S is the singular values

Then we calculated the principal components of the matrix, X:

$$E = S \times V^T \quad Eq 4.3$$

In which E represents the principal components.

Figure 4.19 represents the first principal components for the measured signal when the head and body were steady when the angle between the eye and Doppler sensor was 0°.

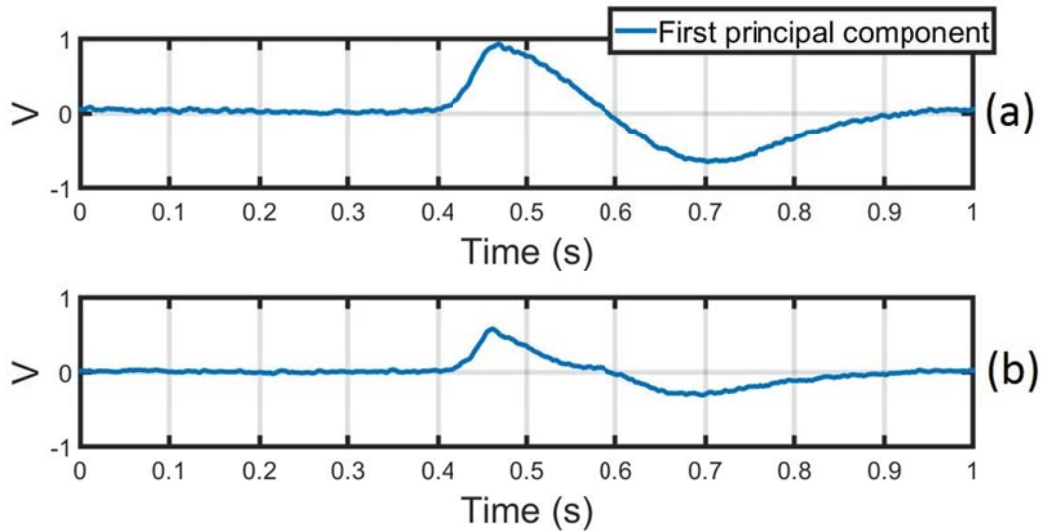


Figure 4.19 First principal components of the signals when the angle between the sensor and the center of eye is 0° : (a) conscious blinking and (b) unconscious blinking.

As we can see the first principal components of each measured signals are exactly the same as obtained data using the arithmetic mean of the signals in the previous section. But because of axis rotations during PCA procedure, the obtained signal for unconscious eyeblink is the inverse of represented signal in figure 4.10.

As the reconstruction procedure for the case when the head and body were not steady, first we selected the first to sixth principal components of each signal and considering the fact that the dominant frequency of eyeblink is near 2 Hz, we chose those selected principal component that have dominant frequency at 2 Hz and then we calculated the mean of them as the reconstructed eyeblink signal. Figure 4.20 and figure 4.21 show the power spectrum of the

first to sixth principal components for both working with computer and walking tasks.

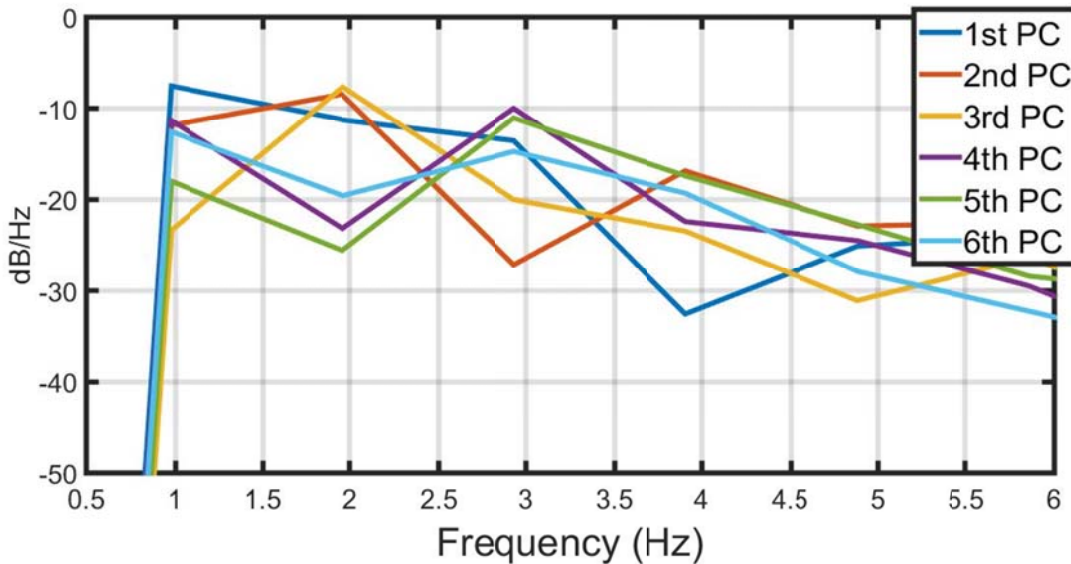


Figure 4.20 The power spectrum of the first to sixth principal components of the signal when the subject sat in front of a personal computer and performed a routine task.

In figure 4.20, the horizontal axis represents the frequency and the vertical axis represents the Power of the signal at each frequency. To better understanding the frequency feature of the signal we selected those frequencies up to 6 Hz. As we can see, the blue, orange and yellow lines associated with the first to third principal components have dominant frequency at 2 Hz and from the experimental results in the previous section, we consider those principal components which have the most of the power at 2 Hz as the representatives for eyeblink. The other principal components have different dominant frequencies and they belong to other movements such as head and body movements. Thus we used this feature for signal separation and we selected the first to third principal components and then we calculated the mean of them as the reconstructed signal as eyeblink.

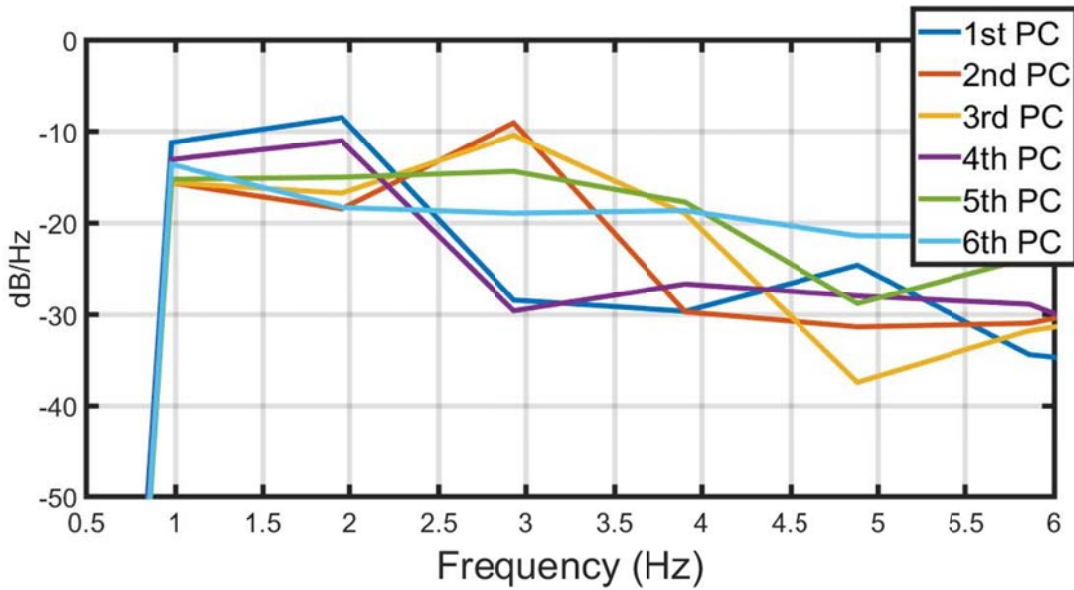


Figure 4.21 The power spectrum of the first to sixth principal components of the signal when the subject performed a walking task.

Figure 4.21 represents the power spectrum of the signal when the subject performed the walking task. In this figure, the horizontal axis represents the frequency and the vertical axis represents the Power of the signal at each frequency and like figure 4.20 to better understanding the frequency characteristics of the signal we selected those frequencies below 6 Hz. As we can see the blue and purple lines associated with the first and fourth principal components have dominant frequency at 2 Hz and they are explaining the eyeblink signal. The other principal components are the representatives of other movements. Therefore as it said before, we selected these signals and calculated the mean of them as the reconstructed signal for eyeblink. Figure 4.22 and figure 4.23 represent the results:

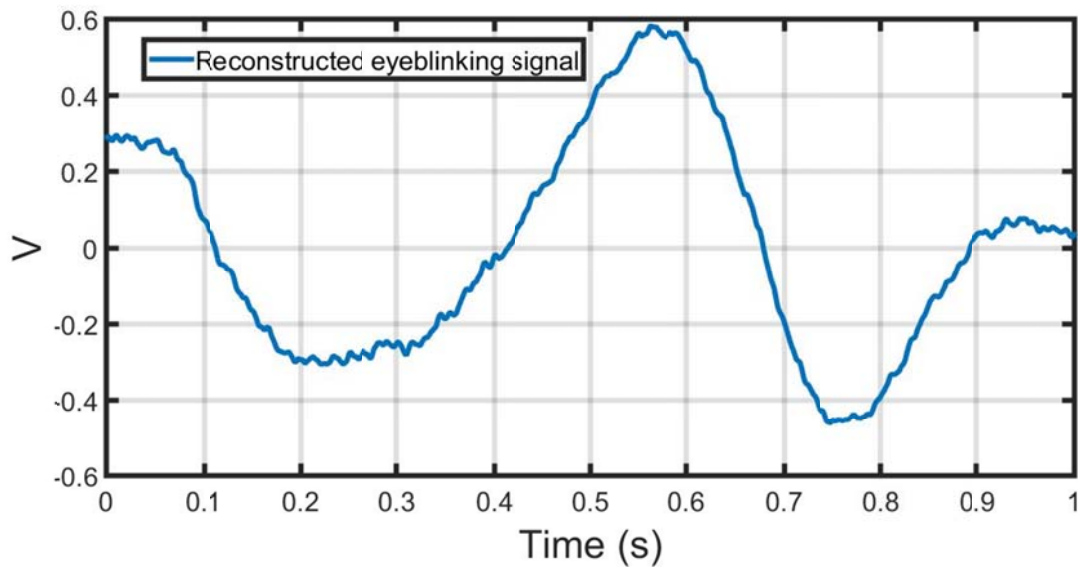


Figure 4.22 Reconstructed blinking signal when the subject sat in front of a personal computer and performing a routine task.

In figures 4.22, the horizontal axis represents the time and the vertical axis represents the normalized amplitude of the signal. Referring back to figure 4.2, the peak of eyeblink signal, measured by Doppler sensor, occurs at the time near 0.5 s. Therefore, considering the size of the waveform and also the time when it occurs, in figure 4.22, which is associated with the blinking signal when the subject sat in front of a personal computer and performed a routine task, we selected the largest wave form between 0.4 to 0.9 s as the eyeblink signal. However due to the phase shift induced by the signal separation procedure the signal may shift slightly toward left or right. As the procedure of eyeblink detection first we defined a threshold value and if the selected signal exceeds this threshold value, the eyeblink is detected. The threshold value for this subject was 0.4 V. Figure 4.24 depicts the eyeblink detection flow.

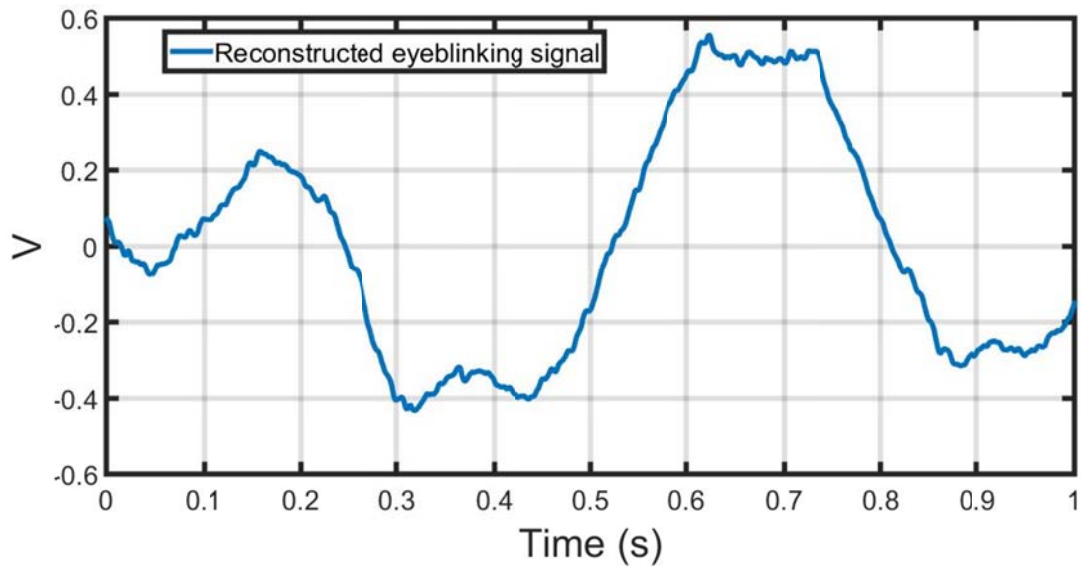


Figure 4.23 Reconstructed blinking signal when the subject performed a walking task.

In figure 4.23, the horizontal axis represents the time and the vertical axis represents the normalized amplitude of the signal. Like figure 4.22 considering the size of the waveform and also the time when it occurs, in figure 4.23, which is associated with the blinking signal when the subject performed a walking task, we selected the largest wave form between 0.52 to 1 s as the eyeblink signal. The procedure of eyeblink detection is the same and the threshold value was 0.4 V. Figure 4.25 shows the eyeblink detection flow for the walking task:

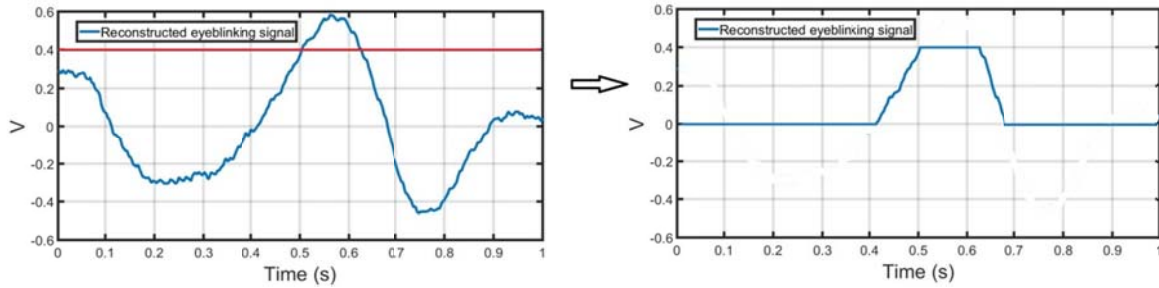


Figure 4.24 Eyeblick detection procedure when the subject sat in front of a personal computer and performing a routine task.

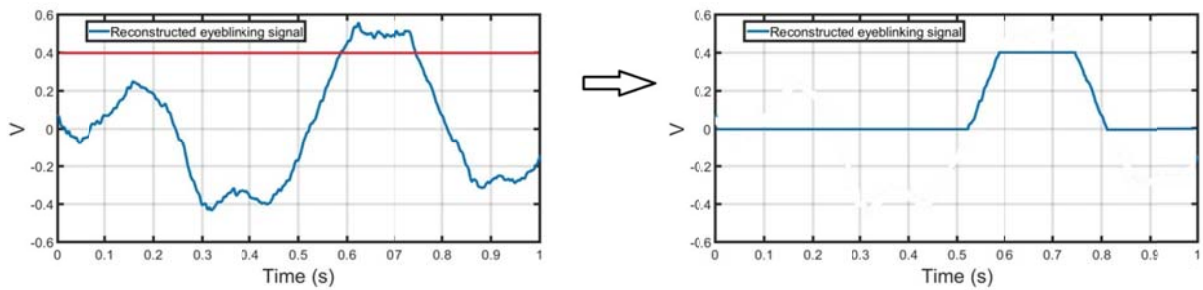


Figure 4.25 Eyeblick detection procedure when the subject performed a walking task.

As we can see in these figures the eyeblick occur because the peak of selected waveforms exceeded the threshold value.

Figure 4.26 to 4.29 depicts the result for the second subject. We observed that the dominant frequency for the second subject was also 2 Hz. The threshold value was also defined 0.4 V.

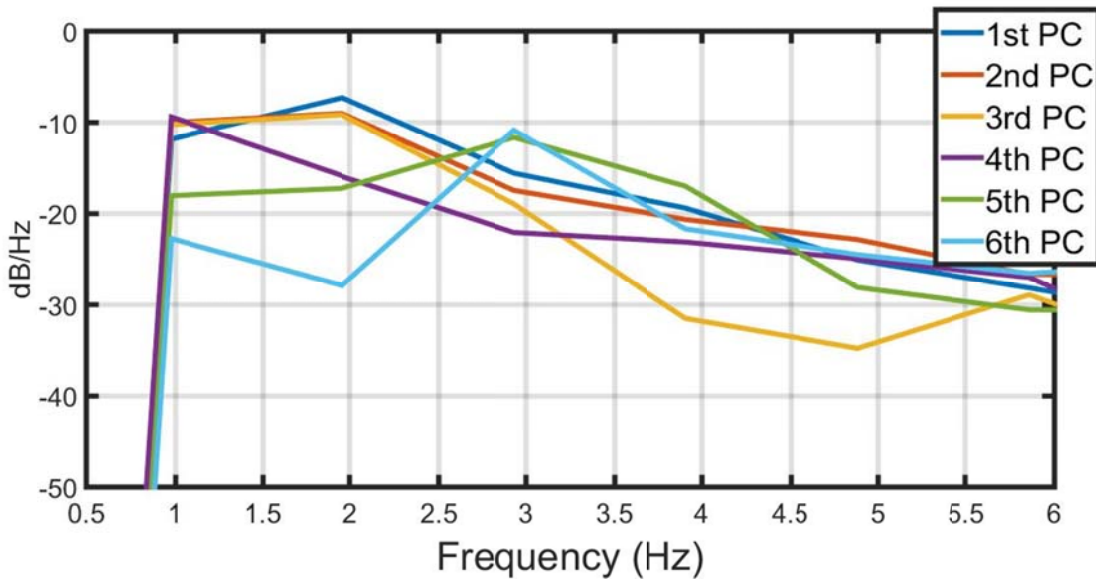


Figure 4.26 The power spectrum of the first to sixth principal components of the signal when the second subject sat in front of a personal computer and performed a routine task.

In figure 4.26, the horizontal axis represents the frequency and the vertical axis represents the Power of the signal at each frequency. As we can see the blue, orange and yellow lines associated with the first to third principal components have a dominant frequency at 2 Hz. Thus we selected the first to third principal components and then we calculated the mean of selected signals as the reconstructed signal for eyeblink during performing the task when the subject sat in front of a personal computer and performed a routine task.

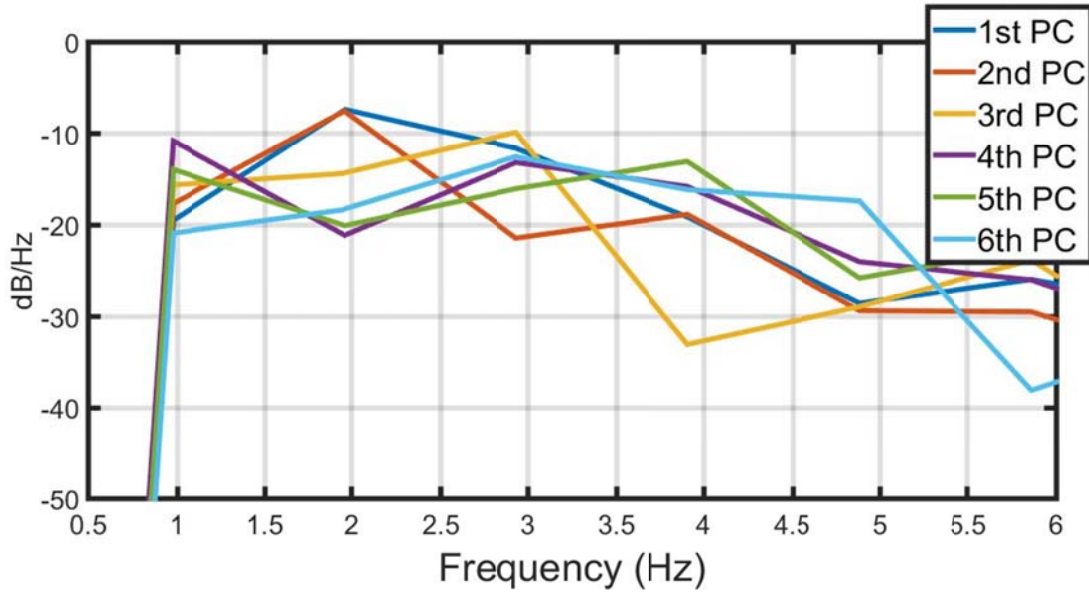


Figure 4.27 The power spectrum of the first to sixth principal components of the signal when the second subject performed a walking task.

In figures 4.27, the horizontal axis represents the time and the vertical axis represents the normalized amplitude of the signal. In this figure the blue and orange lines associated with the first and second principal components have dominant frequency at 2Hz and thus we took the mean of them as the reconstructed signal of eyeblink for the walking task.

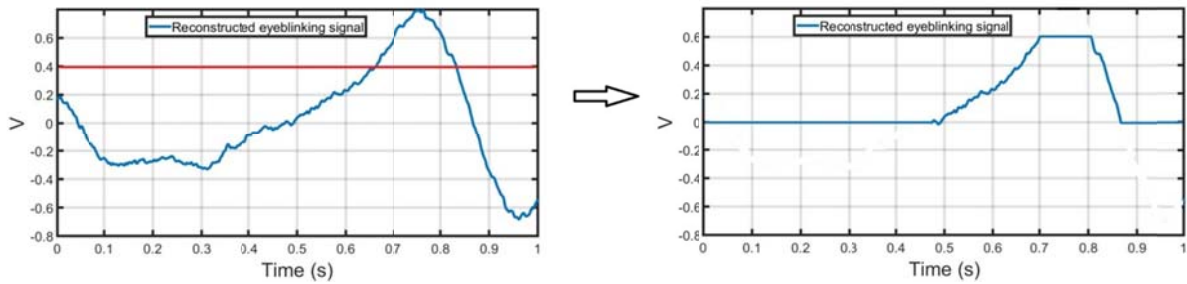


Figure 4.28 Eyeblink detection procedure when the second subject sat in front of a personal computer and performing a routine task.

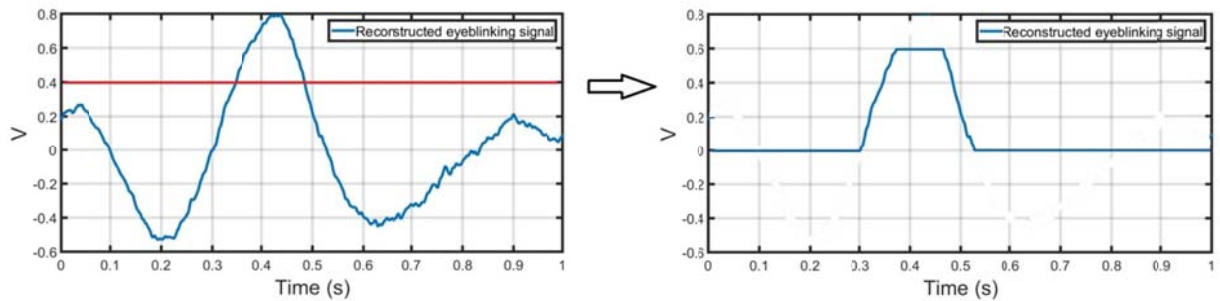


Figure 4.29 Eyeblink detection procedure when the second subject performed a walking task.

In figures 4.28 and 4.29 eyeblink occurs when the selected waveforms for eyeblink exceed the threshold value. In figure 4.28 the selected eyeblink signal is between 0.5 to 1 s and in figure 4.29 it is between 0.3 to 0.82 s. As we can see due to the phase shift during performing the signal separation method the signals are shifted to right and left, respectively.

Chapter 5 Conclusion and future work

In this thesis, we have introduced a glass which can be used for diverse applications such as detecting driver's and pilot's drowsiness and also for measuring several psychophysiological factors. Because it is proposed that eyeblink is a representative for higher nervous processes and it can be used for measuring the level of the cognitive and mental workload during performing tasks. We also introduced an experimental method for eyeblink detection in which we measured eyeblink for both cases when the head and body of the subjects were steady and unsteady. First, we analyzed the frequency characteristics of the eyeblink when the head and body was steady and then we tried to separate the eyeblink signal from the measured signal which was contaminated with the head and body movement using PCA method. We observed that eyeblink measurement is practical when the Doppler sensor was placed in front of the eye, 5 cm away from it, and the angle between the eye and the sensor was between -45° to 45° . The best detectable angle was 0° because the radial velocity at this position has the maximum value. Furthermore, from our experimental results we showed that the Doppler frequency of eyeblink is near 2Hz and this frequency is equivalent to the propose speed of blinking which are [52~138 mm/s] and [24~47 mm/s] for the closing and opening phases, respectively. This frequency may vary from subject to subject. In addition we proposed that the boundary between conscious blinking and unconscious blinking is achievable because the waveforms of the conscious and unconscious blinking are different. Finally, we introduced a method to separate the blinking signal from a signal that had been mixed with head and body movements. This method addresses the advantages of the PCA analysis for pattern recognition and also eyeblink detection. For the feature work we plan to perform the eyeblink detection and also distinguishing the type of it, conscious and unconscious, by using an

appropriate neural network. The results of this work can also be used for the neural network training processes.

Acknowledgments

I wish to dedicate this thesis to my advisor, Professor Masafumi Uchida for his kind, unstinting and endless supports during my research periods at the University of Electro-Communications. I also want to thank my angelic friends, Ali Mokhtari, his sister, Nazila, and his wife, Negar, for their warm supports during my life in Japan. Finally, I need to thank Mr. Inoue for his unswerving supports during my academic life at in japan.

References

- [1] Stern JA and Skelly, J.J. (1984), The eye blink and workload consideration. Proc. Human Factor SOL. 2X: 942-944
- [2] Ohira O (1996), Eyeblink activity in a word-naming task as a function of semantic priming and cognitive load, *Perceptual and Motor Skills*,82,835-842
- [3] Staszek K, Wincza K, and Gruszczynski S (2012), Driver's drowsiness monitoring system utilizing microwave Doppler sensor, in Proc. MIKON, vol. 2, 623–626
- [4] Steven B Ryan, Krystal L Detweiler, Kyle H Holland et al. (2006), A long-range, wide field-of-view infrared eyeblink detector, *Journal of Neuroscience Methods* 152, 74–82
- [5] Kwon K, Shipley R J, Edirisinghe M et al. (2013), High-speed camera characterization of voluntary eye blinking kinematics. *Kinematics. J R Soc Interface* 10: 20130227
- [6] Blumenthal T D, Cuthbert B N, Filion D, Hackley S, Lipp O V and Bortel A V (2005), Guidelines for human startle eyeblink electromyographic studies, *Psychophysiology*, 42
- [7] Hori J, Sakana K and Saitoh Y (2006), Development of a communication Support device controlled by eye movement and voluntary eyeblink, *IEICE TRANS. INF.& SYST.*, VOL E89-D, NO.6
- [8] Liting,W., Xiaoqing, D., Changsong, L.,Wang, K.: Eye Blink Detection Based on Eye Contour extraction. In: *Image Processing: Algorithms and Systems*, SPIE Electronics Imaging, 2009, p. 72450
- [9] Ayudhaya, C., Srinark, T.: A method for a real time eye blink detection and its applications. In: *The 6th International Joint Conference on Computer Science and Software Engineering (JCSSE)*, 2009, pp. 25 – 30
- [10] POLATSEK P (2013), Eye Blink Detection, IIT.SRC, Bratislava, April 23, 2013, pp. 1–8

[11] Ishimaru S, Kunze K, Kise K, Weppner J, Dengel A, Lukowicz P and Bulling A (2014), In the Blink of an Eye – Combining Head Motion and Eye Blink Frequency for Activity Recognition with Google Glass, ACM 978-1-4503-2761-9/14/03

[12] Kim Y (2015), Detection of eye blinking using Doppler sensor with principal component analysis. IEEE antennas and wireless propagation letters, vol. 14, 123-126

[13] Karhunen J and Joutsensalo J (1993), Representation and Separation of Signals Using Nonlinear PCA Type Learning. Neural Networks, Vol 7, No 1, 113-127

[14] Genis Cardona and Noa Quevedo (2013), Blinking and Driving: the Influence of Saccades and Cognitive Workload, Informa Healthcare USA

[15] J. A. VELTMAN and A.W. K. GAILLARD (1998), Physiological workload reactions to increasing levels of task difficulty

Publications and conferences

[1] Amir Maleki, Yuki Oshima, Akio Nozawa, Tota Mizuno, and Masafumi Uchida, Analysis of Fluctuation in Repeated Handwriting Based on Psychophysiological Factors, 7th International Conference on Unsolved Problems on Noise, 21 (2015)

[2] Amir Maleki and Masafumi Uchida, Non-contact measurement of eyeblink by using Doppler sensor, AROB 22nd, 2017

[3] Ryo Hasegawa, Amir Maleki, Masafumi Uchida, Evaluation of Body Sway Using Tactile Stimuli on the Body Trunk, IEEJ Trans., EIS, 136(8), 1135-1141, Aug 2016